Earth Surf. Dynam. Discuss., https://doi.org/10.5194/esurf-2018-13
Manuscript under review for journal Earth Surf. Dynam.
Discussion started: 21 February 2018

Effect of changing vegetation on denudation (part 2): Landscape response to transient climate and vegetation cover

Manuel Schmid [(1)], Todd A. Ehlers[(1)*], Christian Werner.[(2)] ,Thomas Hickler[(2)(3)], Juan-Pablo Fuentes-Espoz[(4)]

[(1)] University of Tuebingen, Department of Geosciences; Wilhelmstrasse 56,
72074 Tuebingen, Germany (Manuel.Schmid@Uni-Tuebingen.de, Todd.Ehlers@Uni-Tuebingen.de)
[(2)] Senckenberg Biodiversity and Climate Research Center (BiK-F), Senckenberganlage 25,
60325 Frankfurt/Main, Germany (Christian.Werner@Senckenberg.de)
[(3)] Department of Physical Geography, Geosciences, Goethe-University, Frankfurt,
Altenhoeferalle 1, 60438 Frankfurt/Main, Germany (Thomas.Hickler@Senckenberg.de)
[(4)] University of Chile, Department of Silviculture and Nature Conservation, Av. Santa Rosa 11315, La Pintana, Santiago RM, Chile (jufuente@uchile.cl)
* Corresponding author: (Todd.Ehlers@Uni-Tuebingen.de)

Earth Surf. Dynam. Discuss., https://doi.org/10.5194/esurf-2018-13
Manuscript under review for journal Earth Surf. Dynam.
Discussion started: 21 February 2018

Abstract We present a numerical modelling investigation into the interactions between transient climate and vegetation cover with hillslope and fluvial processes. Model simulations were designed to investigate the effects of climate change and associated changes in surface vegetation cover on topographic basin metrics such as: slope, relief and channel steepness. The Landlab surface process model was used to evaluate the effects of temporal variations in vegetation cover on hillslope diffusion and detachment limited fluvial erosion. A suite of simulations were conducted to represent present-day climatic conditions and satellite-derived vegetation cover at the four EarthShape study areas as well hypothetical transient long term changes. Two different transient variations in climate and vegetation cover include a step change in climate or vegetation, as well as 100kyr oscillations over 5Myr. Results indicate that the coupled influence of surface vegetation cover and mean annual precipitation shifts basin landforms towards a new steady state, with the magnitude of change highly sensitive to the initial vegetation and climate conditions of the basin. Dry, non-vegetated basins show higher magnitudes of adjustment than basins that are situated in wetter conditions with higher vegetation cover. For coupled conditions when surface vegetation cover and mean annual precipitation change simultaneously, the landscape response tends to be weaker. When vegetation cover and mean annual precipitation change independently from each other, higher magnitude shifts in topographic metrics are simulated. Changes in vegetation cover show a higher impact on topography for low initial surface cover values whereas for areas with high initial surface cover, the effect of changes in precipitation dominate the formation of landscapes. This study demonstrates a sensitivity of catchment characteristics to different transient forcings in vegetation cover and mean annual precipitation, with a crucial role for initial vegetation and climate conditions. Ongoing research is developing fully-coupled landscape evolution and dynamic vegetation model (see companion paper) forced with predicted paleoclimate histories from an atmospheric general circulation model.

Earth Surf. Dynam. Discuss., https://doi.org/10.5194/esurf-2018-13
Manuscript under review for journal Earth Surf. Dynam.
Discussion started: 21 February 2018

1. Introduction

Plants cover most of Earth's surface and interact chemically and physically with the atmosphere, lithosphere and hydrosphere. The abundance and distribution of plants throughout Earth's history is a function, amongst other things, of changing climate conditions that can impact the temporal distribution of plant functional types and vegetation cover present in an area (Hughes, 2000; Muhs et al., 2001; Walther et al. 2002). The physical feedbacks of vegetation on the Earth's near surface manifest themselves mainly through an influence of plants on weathering, erosion, transport and the deposition of sediments (Marston, 2010; Amundson et al., 2015). Although the effects of biota on surface processes has been recognized for over a 100 years (e.g., Gilbert, 1877; Langbein and Schumm, 1958), early studies focused mainly on qualitative descriptions of the underlying processes. With the rise of new techniques to quantify mass transport from the plot- to catchment-scale, and the emergence of improved computing techniques and landscape evolution models, research shifted more towards building a quantitative understanding of how biota influence both hillslope and fluvial processes (Stephan and Gutknecht, 2002; Roering et al., 2002; Marston, 2010; Curran and Hession, 2013). The previous studies motivate the companion papers presented here. In part 1 (Werner et al. 2018-this volume) a dynamic vegetation model is used to evaluate the magnitude of past (Last Glacial Maximum to present) vegetation change along the climate and ecological gradient in the Coastal Cordillera of Chile. Part 2 (this study) presents a sensitivity analysis of how transient climate and vegetation impact catchment denudation. This component is evaluated through implementation of transient vegetation effects for hillslopes and rivers in a landscape evolution model. Together, these two components provide a conceptual basis for understanding how transient climate and vegetation impact catchment denudation.

Previous research in agricultural engineering has focused on plot-scale models to predict total soil loss in response to land-use change (Zhou et al. 2006; Feng et al. 2010) or general changes in plant surface cover (Gyssels et al., 2005), but do not draw conclusions about large-scale geomorphic feedbacks active over longer (millennial) timescales and larger spatial scales. However, a better understanding of how vegetation influences the large scale topographic features (e.g. relief, hillslope angles, catchment denudation) is crucial to understanding the evolution of modern landscapes. At the catchment scale, observational studies have found a correlation between higher values of mean vegetation cover and basin wide denudation rates or topographic metrics (Jeffery et al., 2014; Sangireddy et al., 2016; Acosta et al. 2015). Parallel to the previous observational studies, numerical modelling experiments of the interactions between landscape erosion and surface vegetation cover have also made progress. For example, Collins et al. (2004) were one of the first who attempted to couple vegetation dynamics with a landscape evolution model and found that the introduction of plants to their model resulted in steeper equilibrium landscapes with a higher variability in magnitude of erosional events. Following this, subsequent modelling studies built upon the previous findings with more sophisticated formulations of vegetation-erosion interactions (Istanbulluoglu and Bras, 2005) including the influence of root strength on hillslopes (Vergani et al., 2017). These studies found that not only is there a positive relationship between vegetation cover and mean catchment slope and elevation but there also exists an inverse relationship between vegetation cover and drainage density, due to the plants ability to hinder fluvial erosion and channel initiation.

The advances of the previous studies are limited mainly by their consideration of static vegetation cover or very simple formulations of dynamic vegetation cover. The exception to this is Istanbulluoglu and Bras (2005) who also considered the lag time for vegetation regrowth on hillslopes after a mass wasting event. However, numerous studies (Ledru et al., 1997; Allen and Breshears, 1998; Bachelet et al., 2003) document that vegetation cover changes in tandem with climate change over a range of timescales (decadal to million year). Missing from previous landscape evolution studies, is consideration of not only how transient vegetation cover influences catchment denudation, but also how coeval changes in precipitation influence denudation. While the effects of climate change over geologic timescales on denudation rates and sediment transport dynamics have been investigated by others (e.g., Schaller et al., 2002; Dosseto et al., 2010; McPhillips et al., 2013), the combined effects of vegetation and climate change on catchment denudation have not. Thus, over longer (geologic) timescales, we are left with a complicated situation of both vegetation and climate changes, and the individual contributions of these changes to catchment scale denudation are difficult to disentangle.

In this study, we compliment previous works by investigating both the temporal and spatial sensitivities of landscapes to the coupled vegetation-climate system. By focusing on simplified transient forcings such as a step change, or 100 kyr oscillations in climate and vegetation cover we present a sensitivity analysis of the landscape response to each of these changes, including a better understanding of the direction, magnitude and rates of landscape change. Our model setup is motivated by four study-areas along the climate and vegetation gradient in Chile (Fig. 1a) and illuminates the transient catchment response to biotic vs. climate changes. While we present results representative of four locations in the Coastal Cordillera, Chile, it is beyond the scope of this study to provide a detailed calibration to this area, and save that as a focus of future (ongoing) work as numerous new data sets emerge from the Coastal Cordillera as part of the German EarthShape priority program (www.earthshape.net).

2. Background to model setup

Model setup and the range of initial conditions chosen for models were based upon four study-areas which are located in the Coastal Cordillera of Chile with a latitudinal range from 26ºS to 38ºS. The focus areas shown in Fig. 1a are part of the German EarthShape priority research program (www.earthshape.net) and were chosen because of their similar granitic lithology and geologic and tectonic history (Andriessen and Reutter, 1994; McInnes et al., 1999; Juez-Larré et al., 2010; Maksaev and Zentilli, 1999; Avdievitch et al., 2017), and the large gradient in climate and vegetation cover over the region (Fig.1b,c). These study areas include (from north to south): Parque Nacional Pan de Azúcar; Reserva Santa Gracia; Parque Nacional La Campana, and Parque Nacional Nahuelbuta. Although this study does not explicitly present landscape evolution model results 'calibrated' to these specific areas, we loosely tuned the model input (e.g. precipitation, initial vegetation cover, rate of tectonic rock uplift) to these areas to provide simulation results that would have some relationship to changing vegetation and climate conditions observed on Earth.

Topographic metrics such as mean basin slope, total basin relief, mean basin channel steepness, and mean surface vegetation cover and mean annual precipitation were extracted for the main catchments and a subset of adjacent catchments (Fig. 1a, 1b; Fig. 2). Topographic metrics were extracted from 30m resolution digital elevation model from the NASA shuttle radar topography mission (SRTM), and vegetation related datasets from the moderate resolution imaging spectroradiometer (MODIS) satellite data (https://landcover.usgs.gov/green_veg.php).

Earth Surf. Dynam. Discuss., https://doi.org/10.5194/esurf-2018-13
Manuscript under review for journal Earth Surf. Dynam.
Discussion started: 21 February 2018

3. Methods

3.1. Model Description and governing equations

For this study, we use the open-source model framework Landlab (Hobley et al., 2017), which provides easily accessible methods for building a landscape evolution model. Landlab provides the computational environment to build an experimental set-up to test hypotheses and conduct sensitivity analyses of topography to different surface process parameterizations.

For our study, we chose a model-domain representative of each of the four Chilean areas using an area of 100km^2 which is implemented as a rectangular grid, divided into 0.01km^2 spaced grid cells. For simplification in the presentation of results, we present our results for the driest, northern most area (Parque Nacional Pan de Azucar) and for the Parque Nacional La Campana which is situated at 32°S Latitude (Fig.1) and shows the highest values in analyzed basin metrics (Fig. 2), although the general behavior and results presented here are representative of the other two areas not shown. The topographic evolution of the landscape is a result of tectonic uplift and surface processes, incorporating detachment limited fluvial erosion and diffusive transport of sediment across hillslopes (Fig.3). These processes are linked to, and vary in their effectiveness due to surface vegetation density. Details of the implementation of these processes into Landlab are explained in the following subsections.

This model setup is simplified in regards to hydrological parameters like, for example, soil moisture and groundwater and unsaturated zone flow. Also, the erosion and transport of material due to mass-wasting processes such as rockfalls and landslides are not considered. We argue that those processes do not play a major role in the basins we used for model-calibration and that the processes acting continuously along hillslopes and channels have the largest impact on shaping our reference landscapes. Additional caveats and limitations of the modeling approach used are discussed in Section 5.4. Main model parameters used in the model (and described below) are provided in Table 1.

3.2. Boundary and Initial Conditions, and Model Free Parameters

In an effort to keep simulations for the different EarthShape areas comparable, we minimized the differences in parameters between simulations. The exceptions to this include the surface vegetation cover and mean annual precipitation, which were varied between simulations. One of the main controls on topography is the rock uplift rate. We kept the rock uplift rate temporally and spatially uniform across the domain and at 0.2 mm/yr (Table 1). Studies of the exhumation and rock uplift history of the Coastal Cordillera, Chile, are sparse at the latitudes investigated here, but existing and in progress studies further to the north are broadly consistent with the rock uplift rate used here (Juez-Larré et al., 2010; Avdievitch et al., 2017). Furthermore, the thermochronometer cooling ages in the northern Coastal Cordillera suggest constant Cenozoic exhumation over >50 Ma at this rate. Thus, despite being located on an active plate boundary, existing observations suggest relatively slow, and temporally constant rock uplift of this region.

The initial topography used in our simulations was a random white-noise topography with <1 m relief. To avoid unwanted transients related to the formation of this initial topography we conduct equilibrium simulations for each set of the different climate and vegetation scenarios (see below), and run the model for 15 Myr until a topographic steady-state is reached. The equilibrium topography after 15 Myr was used as the input topography for subsequent experiments that impose transient forcings in climate, vegetation, or both (Fig. 4). The model simulation time shown in subsequent plots is the time since completion of this initial 15 Myr steady-state topography development. In the results section, we present these results starting with differences in the initial steady-state topographies (prior to imposing transient forcings) and then add different levels of complexity by imposing either: (1) a single transient step-change for the vegetation cover (Fig. 4b); (2) a step change in the mean annual precipitation (Fig. 4d); (3) 100 kyr oscillations in the vegetation cover (Fig. 4a); (4) 100 kyr oscillations in the mean annual precipitation (Fig. 4c); or (5) 100 kyr oscillation in both the vegetation cover and mean annual precipitation (both Fig. 4a and 4c). This approach was used to produce a stepwise increase in model complexity for evaluating the individual, and then combined, effects of fluvial and hillslope processes to different forcings.

The magnitude of induced rainfall transient forcings where based upon the present-day conditions along the Coastal Cordillera study areas (Fig. 1b, c). The step change and oscillations in vegetation cover and mean annual precipitation imposed on the experiments were designed to investigate vegetation and precipitation change effects on topography over the last ~0.9 Ma, the period during which a 100 kyr orbital forcing is dominant in Earth's climate. Given this timescale of interest, we impose a 10% magnitude change in the step-increase or decrease, or the amplitude change in oscillations for the vegetation cover. This magnitude of vegetation cover change is supported by dynamic vegetation modeling of vegetation changes over glacial-interglacial cycles in Chile (see companion paper by Werner et al. 2018-this journal) and to some degree elsewhere in the world (Allen et al., 2010; Prentice et al., 2011; Huntley et al., 2013). We assume that the present-day conditions of combined vegetation cover and mean annual precipitation along the north-south gradient of the coastal cordillera are directly linked (Fig. 1b, c), and therefore follow an empirical approach based on the present day mean annual precipitation vs. vegetation cover relationship in Chile (Fig. 5). We do this by associating each 10% change in vegetation cover (dV) with a corresponding change of mean annual precipitation (dP, Fig. 5) present in the study areas considered.

The boundary conditions used in the model were the same for all simulations explained above (Fig. 3). One boundary was held at a fixed elevation and open to flow outside the domain. The other three were allowed to increase in elevation and had a zero-flux condition. This design for boundary conditions is similar to previous landscape evolution modeling studies (Istanbulluoglu and Bras, 2005) and provides a means for analyzing the effects of different vegetation cover and precipitation forcings on the individual catchment and subcatchment scale.

3.3. Vegetation Cover Dependent Geomorphic Transport Laws

The governing equation used for simulating topographic change in our experiments follows the continuity of mass. Changes in elevation at different points of the model domain over time dz(x,y,t) depend on

$$\frac{\delta z(x,y,t)}{\delta t} = U - k_d \nabla z - D_c \tag{1}$$

where z is elevation, x, y are lateral distance, t is time, U is the rock uplift rate , $k_d \nabla z$ the linear diffusive flux of sediment along hillslopes, and D_c the detachment capacity of channels (Tucker et al., 2001a). Our implementation of vegetation cover effects for the last two parameters in the Landlab model are described in more detail below.

3.3.1 Vegetation Cover Influenced Diffusive Hillslope Transport

The change of topographic elevation in a landscape over time which is directly caused by hillslope-dependent diffusion can be characterized as:

$$\frac{\delta z}{\delta t} = -\nabla q_{sd} \tag{2}$$

Earth Surf. Dynam. Discuss., https://doi.org/10.5194/esurf-2018-13
Manuscript under review for journal Earth Surf. Dynam.
Discussion started: 21 February 2018

Landscape evolution models characterize the flux of sediment q_s either as a linear or non-linear function of surface slope S (Culling, 1960; Fernandez and Dietrich, 1997). In order to keep the number of free parameters for the simulation to a minimum, we used the linear description of hillslope diffusion:

$$q_{sd} = K_d S \tag{3}$$

Following the approach of (Istanbulluoglu and Bras, 2005), we assign the linear diffusion coefficient K_d as a function of surface vegetation density V, an exponential coefficient α, and a baseline diffusivity K_b, such that:

$$K_d = K_b e^{-(\alpha V)} \tag{4}$$

3.3.2 Vegetation Cover Influence on Overland Flow and Fluvial Erosion

The erosion and transport of material due to river incision is represented as a detachment-limited process

$$\frac{\delta z}{\delta t} = K_v A^m S^n - E_{threshold} \tag{5}$$

where the amount of lowering of elevation (z) over time depends on the fluvial erodibility K_v, [L^{1-2m} t^{-1}] (a function of soil type, climate, vegetation and the scaling of runoff to drainage area). The contributing drainage area to each node is represented by A [L^2], S is the corresponding channel slope, and *m*, and *n* are empirically derived constants (Howard and Kerby, 1983; Whipple and Tucker, 1999). The detachment-limited erosion law can be re-written in a form that directly links excess bed shear stress to detachment capacity of a river where:

$$D_c = k_e(\tau_b - \tau_c)^p \tag{6}$$

$$\tau_b = \rho_w g R S \tag{7}$$

where k_e represents the erodibility of the substrate, τ_b represents the bed shear stress acting on the bed surface, τ_c is the critical shear stress needed to erode the substrate, ρ_w is the density of water, g is gravitational acceleration, R is hydraulic radius and S is local channel slope. By combining the shear-stress formulation with Mannings equation and introducing two Mannings surface roughness values (n_V for the influence of vegetation on surface roughness and n_s for the influence of the soil surface to surface roughness, e.g., Istanbulluoglu and Bras, 2005) we can reformulate the hydraulic radius R (Wilgoose et al., 1991; Istanbulluoglu et al., 2004) and write the shear-stress formulation as a function of the Mannings coeffcients:

$$\tau_f = \rho_w g(n_s + n_v)^{\frac{6}{10}} q^m S^n \tag{8}$$

By writing n_v as a function of a basic Mannings coefficient for a reference vegetation cover n_{vr} and V_r, the vegetation cover at each individual node V and an empirical scaling parameter W, we arrive at:

$$n_v = n_{vr}\left(\frac{V}{V_r}\right)^W \tag{9}$$

Combining equation 8 and 9 results in an equation for vegetation cover dependent shear stress at each node. The effects of surface vegetation cover on both diffusivity and fluvial erodibility are shown in Figure 6.

3.4 Model Evaluation

Model performance was evaluated using the above equations and different initial vegetation covers and mean annual precipitation based on the steady-state predicted topography. Our focus in this study is on the general surface process response to different transient vegetation and climate conditions, rather than a calibrated modeling study of the Chilean study areas. Nevertheless, topographic metrics of relief, mean slope, and normalized steepness index(K_{sn}) were computed from the model results and compared to observed values from the 30 m SRTM DEM for each of the four areas (Fig. 2).

Earth Surf. Dynam. Discuss., https://doi.org/10.5194/esurf-2018-13
Manuscript under review for journal Earth Surf. Dynam.
Discussion started: 21 February 2018

This was done to evaluate if our implementation of the governing equations in Section 3.4 produced topographies within reason of present day topographies in the four Chilean areas. A more detailed model calibration is beyond the scope of this study, and not meaningful without additional observational constraints on key parameters such latitudinal variations in the rock uplift rate and erosivity.

4. Results

Our presentation of results is structured around three groups of simulations. These include: 1. steady-state simulations where equilibrium topographies are calculated for different magnitudes of vegetation cover and identical precipitation forcing. A second set of steady-state simulations with the same magnitudes vegetation cover as 1. but with different precipitation forcings corresponding to each vegetation cover (Section 4.1). 2. Simulations with a transient step-change in either surface vegetation density or precipitation (Section 4.2) that is initiated after the landscape has reached steady state. and 3. simulations with a transient 100 kyr oscillating time series of changing vegetation or precipitation that occurs after the landscape has reached steady state (Section 4.3). For each group of transient simulations, we show the topographic evolution with help of standard topographic metrics and the corresponding erosion rates after the induced change.

4.1 Equilibrium Topographic Metrics

Topographic metrics from each of the four Chilean focus areas (Fig. 1a) were extracted for comparison to equilibrium topographies predicted after 15 Myr of model simulation time. This comparison was done to document the model response to changing vegetation cover (with climate held constant) and changing vegetation cover and precipitation, and also to demonstrate the modeling approach employed throughout the rest of this study captures the general characteristics of different topographic metrics along the Chilean Coastal Cordillera. We refrain from conducting a more detailed model-observation comparison for reasons previously mentioned.

Analysis of the digital elevation model for each of our four Chilean focus areas illustrates observed changes in catchment relief, slope, and channel steepness (K_{sn}) in relation to the surface vegetation (Fig. 7, red points) and latitude (Fig. 2). The general trend in the observed metrics shows a non-linear increase in each metric until a maximum is reached for regions with 70% vegetation cover. Following this, all observed metrics show a decline towards the area with 100% vegetation cover.

The model predicted equilibrium topographies (Fig. 7a,b,c) from four different steady-state simulations with variable vegetation cover but a constant mean annual precipitation (900 mm/yr) show a nearly linear increase in all observed basin metrics with increasing vegetation cover and therefore do not reflect the overall trend observed in the DEM from the study areas. For example, basin relief and slope are both under predicted for simulations with $V < 100\%$ (Fig.7a,b), and only the predicted maximum relief for a fully-vegetated simulation resembles the DEM maximum value. For the normalized channel steepness, only two observed mean values (for $V = 10\%$ and 70%) lie within the range of mean to maximum predicted Ksn values (Fig.7c).

The resulting equilibrium topographies from simulations with both variable mean annual precipitation and vegetation cover (Fig.7d,e,f) show an improved representation of the general trend of the DEM data. The vegetation cover and precipitation values used in these simulations come from the values observed in the Chilean areas (Fig. 1b, c; Fig. 5). In these simulations, the maximum in the observed basin metrics is situated at values of $V = 30\%$ with a following slight

Earth Surf. Dynam. Discuss., https://doi.org/10.5194/esurf-2018-13
Manuscript under review for journal Earth Surf. Dynam.
Discussion started: 21 February 2018

decrease in the metric for V = 30% to V = 70%, followed by a steeper decrease in metrics from V = 70% to V = 100%. Generally the model-based results tend to underestimate the basin relief and overestimate the basin channel steepness (Fig.7d,f). Variations in basin slope are captured for all but the non-vegetated state (Fig.7e).

Although the above comparison between the models and observations demonstrates a range of misfits between the two, there are several key points worth noting. First, the model results shown are highly simplified in their setup (e.g. assuming similar rock uplift rate, identical lithology and constants), and assume the present day topography is in steady state for the comparison. Second, despite the previous simplifying assumptions, the degree of misfit between the observations and model are surprisingly small when both variable vegetation and variable precipitation, are considered (Fig. 7d,e,f). Finally (third), the general 'humped' shape curve observed in the Chilean areas is captured in the model predictions (Fig. 7d,e,f), with the notable exception that the maximum in observed values occurs at a higher vegetation cover (V = 70%) than the model predictions (V = 30%). Explanations for the possible source of these differences are revisited in the discussion section. Without additional observations from the Chilean areas, reduction of the misfit between the observations and models is not tractable.

4.2 Transient Topography – Step Change

The evolution of our model topographies after a induced instantaneous disturbance (Fig. 4) of either only the surface vegetation cover (Fig. 8, green lines) or a step change in only the mean annual precipitation (Fig. 8, blue lines) is analyzed for changes in topographic metrics for either a positive disturbance (Fig. 8a,b,c) or a negative disturbance (Fig.8d,e,f). This scenario with changes in only vegetation or only precipitation was chosen to analyze sensitivity of drainage basins to changes in vegetation cover and precipitation and isolate the effects of these specific transient forcings. Decoupling of vegetation and climate changes can occur via sudden disturbances, such as wildfires and lagged vegetation responses to climatic changes. Mean catchment erosion rates are also analyzed for their evolution after the disturbance (Fig.9). For simplicity in presentation, results are shown for only two of the initial vegetation (V) and precipitation (P) values for vegetation covers of 10 and 70%, and precipitation rates that correspond to these vegetation covers (i.e. P(V=10%) or P(V=70%)) in the Chilean areas (Fig. 5). The results described below show a general positive correlation between all observed topographic metrics and surface vegetation cover and a negative correlation between observed topographic metrics and mean annual precipitation and therefore supports the data from our equilibrium topography simulations. The adjustment time until the system again reaches a new steady state varies between different simulations.

4.2.1 Positive Step Change in Vegetation Cover or Precipitation

Topographic Analysis

A positive step change in vegetation cover (V) from V = 10% to V = 20% (solid green line Fig. 8a,b,c) leads to an increase of mean basin relief from 270m to 520m, mean basin slope from 11.2° to 15.9°, and mean basin channel steepness from 108m$^{-0.9}$ to 222m$^{-0.9}$, which corresponds to a factor 1.9, 1.42, and 2.1 change, respectively. The adjustment time until a new steady state in each metric is reached is 3.1Ma. The corresponding positive change in mean annual precipitation (solid blue lines, Fig. 8a,b,c) leads to a decrease of mean basin relief to 176m, mean basin slope to 8.6° and mean basin channel steepness to 67m$^{-0.9}$. This corresponds to a decrease by factors of 1.5, 1.2 and 1.6, respectively. The adjustment time to new steady state conditions in this case are shorter and 1.1Ma (Fig.8a,b,c). A second feature of these results is the brief increase and then decrease in basin average slope angles following the step change (Fig. 8b).

For simulations with V = 70% initial surface vegetation cover, a positive increase to V = 80% leads to an increase of mean basin relief from 418m to 474m, mean basin slope from 15.5° to 16.8° and mean basin channel steepness from 172$m^{-0.9}$ to 199$m^{-0.9}$. This causes an increase in each metric by factors of 1.1, 1.1 and 1.2, respectively. The adjustment time to steady-state conditions is 1.9Ma (dotted green lines, Fig 8a,b,c). The corresponding positive change in mean annual precipitation leads to a decrease of relief to 268m, decrease in slope to 11.9° and decrease of channel steepness to 105$m^{-0.9}$. This resembles a decrease by factors 1.5, 1.3, 1.6, respectively. Adjustment time in this case is 1.7Ma (dotted blue lines, Fig. 8a,b,c). The basin slope data shows similar behavior as the V_{ini} = 10% simulations with an initial decrease and then increase for a vegetation cover step change and an initial increase and then decrease for a step change in mean annual precipitation. Comparison of the change in the topographic metrics for the low (V=10%) and high (V=70%) initial vegetation covers, the magnitude of change in each metric is larger when the step change occurs on a low, rather than higher, initial vegetation cover topography.

Erosion Rate Changes

Erosion rates show instantaneous reactions to positive disturbances in vegetation or precipitation. Generally, the model results show a negative relationship between increases in vegetation cover and erosion rates and a positive relationship between increases in precipitation and erosion rates. Although the reaction between the disturbances and changes in erosion rates are instantaneous, the specific maximum or minimum is reached after some lag time and the magnitude and duration of non-equilibrium erosion rates varies between different simulation setups.

For initial vegetation cover of V = 10%, a change in vegetation cover (dV) of +10% leads to a decrease in erosion rates from 0.2 to 0.03mm/yr (factor of 5.7 decrease, Fig. 9a green line). The minimum erosion rate is reached 43.5kyrs after the step change occurs. Following this minimum in erosion rates, the rates increase until the steady-state erosion rate is reached after the adjustment time. An increase in mean annual precipitation corresponding to a vegetation cover of 10% (i.e. P(V=10%) to P(V=20%); Fig. 5) leads to an increase in erosion rates to a maximum of 0.44mm/yr after 74.8kyrs (factor of 2.2 increase, Fig.9a, blue line). For initial vegetation of V = 70% a vegetation increase of dV = +10% results in minimum erosion rates of 0.14mm/yr after 117.7kyrs (factor of 1.4 decrease, Fig. 9b, green line). A corresponding increase in precipitation for these same vegetation conditions leads to maximum erosion rates of 0.44mm/yr after 107.5kyrs which is an increase by a factor of 2.2 (Fig.9b, blue line). The previous results for a positive step change in vegetation or precipitation demonstrate that the magnitude of change in erosion rates is large for changes in precipitation rate than for vegetation cover changes, and in low initial vegetation cover settings (V=10%) that magnitude of change in erosion rates for changing vegetation is larger (compare green lines Fig. 9a with 9b).

4.2.2 Negative Step Change in Vegetation Cover or Precipitation

Topographic Analysis

For negative step-changes in vegetation (green curves, Fig. 8d,e,f), the results show a sharp decrease in topographic metrics associated with shorter adjustment times compared to the positive step change experiments (compare Fig. 8d,e,f with a,b,c). For step changes in precipitation (blue curves, Fig. 8d,e,f), the increase of topographic metrics happens slower and therefore with longer adjustment times. A negative step change in vegetation cover from V = 10% by dV = -10% leads to a decrease of mean basin relief from 269m to 35m, mean basin slope from 11.2° to 2.3° and mean basin channel steepness from 108$m^{-0.9}$ to 11$m^{-0.9}$ which resembles decreases by factors of 7.8, 3.8 and 9.6. The adjustment time until a new steady-state is reached is 0.26Ma (solid green lines, Fig. 8d,e,f). The corresponding negative change in precipitation leads to an increase in mean basin relief to 512m, mean basin slope to 15.8° and mean basin channel steepness to 223m$^{-0.9}$. These increases reflect changes by factors of 1.9, 1.4 and 2.1 with an adjustment time of 4.9Ma (dotted green lines, Fig.8d,e,f). Mean basin slope results (Fig. 8e) for a step change in vegetation illustrate a pulse-like feature of initially increasing slope values, followed by a decrease to lower slope values. In contrast, a negative step change in precipitation induce an initial decrease in slope, followed by a gradual increase in slope to a value higher than was initially observed before the change.

Simulations with initial vegetation cover V = 70% and dV = -10% show a decrease in mean basin relief from 418m to 356m, mean basin slope from 15.5° to 13.6° and mean basin channel steepness from 172m$^{-0.9}$ to 144m$^{-0.9}$ which resembles changes by factors of 1.2, 1.1 and 1.2 and an adjustment time of 2.1Ma (dotted green lines, Fig.8d,e,f). Corresponding negative changes in precipitation lead to increase of basin relief of 465m, basin slope to 16.4° and channel steepness to 195m$^{-0.9}$ which resembles changes by factors of 1.1 for all three values. Adjustment time in this case is 2.2Ma (dotted blue lines, Fig.8d,e,f). Behavior of mean basin slope after the step-change follows the V = 10% simulations but shows lower amplitudes of basin slope for both step-changes in vegetation and precipitation.

Erosion Rates

The positive step-change results (Fig. 9a, b) indicated that erosion rates reach their minimum or maximum after a lag time after the change, and show significant differences in the magnitude and duration of non-equilibrium conditions depending on if vegetation or precipitation were changing. Simulations with a decrease from V = 10% to V = 0% (Fig. 9c) show a sudden increase in erosion rates to a maximum value of 3.5mm/yr which is an increase from steady state conditions by a factor of 17.7 which is reached after 19.5kyrs (green line, Fig.9c). A step decrease in precipitation for this corresponding vegetation difference (i.e. P(V=10%) to P(V=0%) leads to a smaller, and protracted (longer adjustment time) decrease in erosion rates to 0.03mm/yr after 50.1kyrs. These conditions cause a factor of 5.6 decrease (blue line, Fig. 9c). Simulations of V = 70% with a vegetation change of dV = -10% show an increase in erosion rates to 0.27mm/yr which is a factor of 1.4 increase after 126.3kyrs (Fig. 9d). For the corresponding decrease in precipitation the data show a decrease in erosion rates to 0.15mm/yr after 124.5kyrs. This resembles change by factor of 1.2 (blue line, Fig. 9d).

4.3 Transient Topography – Oscillating

In addition to simulations where a transient step-change in either surface vegetation density or mean annual precipitation was conducted, we set up two distinct sets of simulations with an oscillating transient signal with a period of 100kyrs. This period resembles the eccentricity driven part of the Milankovitch cycle that is dominant in Earth's climate over the last 0.9Ma.

4.3.1 Oscillating Surface Vegetation Cover, Constant Precipitation

Topographic Analysis

The topographic evolution in simulations with a constant precipitation (10 and 360mm/yr for V=10%, and V=70%, respectively) and oscillating vegetation cover show a different response than the previous step change experiments. The differences depend on the initial steady-state vegetation cover prior to the onset of 100kyr oscillations. All observed basin metrics (Fig. 10) show an initial oscillating decrease in values until a new dynamic steady-state is reached where the amplitude in oscillations is less than in the preceding initial adjustment period. Simulations with V = 10% (Fig. 10a) show a decline in the basin relief from 269m to 107m which resembles a decrease of the mean elevation of factor 2.5. The positive amplitude of oscillation is 9m, the negative amplitude is 8.3m but time intervals of negative amplitudes are longer

Earth Surf. Dynam. Discuss., https://doi.org/10.5194/esurf-2018-13
Manuscript under review for journal Earth Surf. Dynam.
Discussion started: 21 February 2018

compared to positive amplitudes. For simulations with V = 70% the reaction and adjustment to the new dynamic steady-state is less pronounced with a decline in relief from 410m to 407m (Factor 1.01) with positive and negative amplitudes in dynamic steady-state of 1.6m. Analysis of mean basin slope for the model topographies with low (V=10%) vegetation shows a similar behavior with a decrease of the mean slope from 11.2° (prior to the onset of oscillations) to 6.0° (Factor 1.6, Fig. 10b). However, before this new equilibrium is reached, the slopes show an increase in mean slope for the first two periods of vegetation oscillation which then declines towards the new long-term stable dynamic equilibrium which is reached after approximately 500kyrs. Local maxima of mean basin slope coincide with local minima in basin relief. For the V = 70% simulations, the reaction is significantly smaller with no change in mean slope for the new dynamic equilibrium and amplitudes of both positive and negative of 0.16°. Mean basin channel steepness (Fig. 10c) reflects the behavior of mean basin elevation. For V = 10% simulations the mean channel steepness decreases from values of $108m^{-0.9}$ to $40m^{-0.9}$ (factor 2.7 change) with a positive amplitude of $3.7m^{-0.9}$ and a negative amplitude of $6.1m^{-0.9}$. For V = 70% simulations the response is again only minor, compared to the lower initial vegetation cover simulations with a change of mean channel steepness from $186m^{-0.9}$ to $167m^{-0.9}$ and positive amplitudes of $1.1m^{-0.9}$ and negative amplitudes of $0.9m^{-0.9}$. Like the elevation data, the steepness data shows a distinct oscillating pattern with slow increases to local maxima and rapid decreases to local minima which coincide with maxima/minima of elevation data. Taken together, the previous observations demonstrate a larger change in topography for oscillations in poorly vegetated areas compared to those with higher vegetation cover. Furthermore, the magnitude of topographic change that oscillations in vegetation impose on topography are largest in the first ~500 kyr after the onset of an oscillation, and diminish thereafter.

Erosion Rates

The erosion history for simulations with oscillating vegetation cover (Fig. 11) demonstrate large variations in the erosion rate that depend on the average vegetation cover of the oscillation. Furthermore, pronounced differences in the amplitude of erosion occur if the vegetation cover is above or below the mean of the oscillation (Fig. 4a). More specifically, simulations with V = 10% show a pattern of a small decrease in erosion rates (from 0.2 to 0.03mm/yr) when vegetation cover increases above the mean cover, in contrast to a large increase in erosion rates up to 3.3mm/yr when vegetation cover decreases below the mean of the oscillation (Fig. 2, Fig. 11). Maximum erosion rates decline over multiple periods of oscillation until they reach a dynamic steady-state with maximum rates of 1.2mm/yr at 760kyrs after the onset. Time periods of higher erosion rates (>0.2mm/yr) have a mean duration of 28kyrs, whereas periods of lower erosion rates (<0.2mm/yr) have a mean duration 72kyrs. For simulations with high vegetation cover (V = 70%) the maximum and minimum erosion rates are 0.28 and 0.15mm/yr, respectively. The magnitude of maximum and minimum erosion rate are not significantly time-dependent and are reached at each local vegetation cover minimum. The mean duration of periods with higher erosion rates (> 0.2mm/yr) is 55kyrs whereas the duration for periods with lower rates (< 0.2mm/yr) is 45kyrs. These results demonstrate that areas with low vegetation cover experience not only larger amplitudes of change in erosion rates, but also an asymmetric change whereby decreases in erosion rates are lower magnitude than the increases in erosion rates.

4.3.2 Oscillating precipitation, Constant Vegetation

Topographic Analysis

The evolution of topographic parameters for simulations with oscillating mean annual precipitation and constant surface vegetation cover (V=10 or 70%, Fig. 12) show a less extreme and smaller temporal change in erosion rate to variations in precipitation compared to the previous discussed effects of oscillating vegetation cover (Fig. 11). In Fig. 12a, the mean basin relief results for V = 10% and oscillating precipitation show small variations (+4.9m to -3.8m) in relief around a mean of 269m, which is similar to the mean relief prior to the onset of oscillations at 5000kyrs. For simulations with V = 70% the change in relief is slightly more pronounced with adjustment to a new mean of 380m from 418m in steady-state conditions. This change in mean relief equates to factor of 1.1 change. The evolution of topographic slope (Fig. 12b) for V = 10% simulations shows an adjustment to a new dynamic equilibrium from 11.2° to 10.6° (Factor 1.05) with a negative amplitude of 1.2° and positive amplitude of 0.9°. For V = 70% the mean slope values do not significantly change from steady-state to transient conditions and the amplitudes of oscillation are 0.6° (positive) and 0.7° (negative). Mean channel steepness (Fig. 12c) for V=10% shows an adjustment from 108$m^{-0.9}$ to 110$m^{-0.9}$ (Factor 1.01). The amplitude of oscillation is 4 $m^{-0.9}$ for both negative and positive amplitudes. For V_{ini} = 70% simulations the topography adjusts from 171$m^{-0.9}$ to 152$m^{-0.9}$ (Factor 1.1) with amplitudes of 4.5$m^{-0.9}$ for both positive and negative changes. Thus, although Figure 12 illustrates changes in topographic metrics that result from oscillations in precipitation occurring around vegetation covers of 10 and 70%, these changes are significantly smaller than those predicted for constant precipitation, but oscillating vegetation conditions (Fig. 10).

Erosion Rates

Predicted erosion rates from simulations with constant surface vegetation cover and oscillating mean annual precipitation indicate different amplitudes of change around the mean erosion rate depending on the vegetation cover. For simulations with V = 10% (Fig. 13, blue solid line) erosion rates oscillate symmetrically around the steady-state erosion rate of 0.2mm/yr. The maximum and minimum erosion rates of 0.42 and 0.01mm/yr, respectively, result in no change in the mean rate. In contrast, predicted rates with a higher vegetation cover of V = 70% (Fig. 13, blue dotted line) demonstrate an asymmetric oscillation in rates around the mean, whereby the maximum in rates (0.43mm/yr) has a larger difference above the mean rate, then do the minimums in the oscillation (0.12mm/yr). For this higher vegetation cover scenario, a gradual increase in the mean erosion rate from 0.2 to 0.25 mm/yr as time progresses is evident. Furthermore, the maximum and minimum erosion rates decline over several oscillation periods to values of 0.38 and 0.15mm/yr, respectively. Taken together, these results indicate that oscillations in precipitation impact erosion with different magnitude depending on the amount of vegetation cover. Areas with low vegetation cover demonstrate the highest and symmetric oscillation of erosion rates due to changes in precipitation whereas in areas with high vegetation cover the effect of negative changes in precipitation is dampened by vegetation.

5. Discussion

The previous results highlight predicted topographies with different sensitivities to changes in either surface vegetation cover or mean annual precipitation. The previous simulations, were conducted to isolate the magnitude of effect each parameter has on topography and erosion. In the following, we synthesize the previous results and then build upon them to discuss the, over longer time-scales, more common scenario of synchronous variation in both precipitation and vegetation cover.

5.1 Interpretation of Steady-State Simulations

Landscapes in a topographic steady-state show distinct features in topographic metrics that are widely used to estimate catchment-averaged erosion rates and therefore the leading processes of erosion within a landscape (DiBiase et al., 2010). In most studies, focusing on comparing *in-situ* measured ^{10}Be erosion rates with topographic metrics, this is done in catchments with low variations in precipitation to focus on distinct topographic controls on soil erosion and transport processes. By conducting simulations with equal soil properties and assuming that the basic processes of sediment erosion and transport do not change between different climate-settings we can reproduce (Fig. 7) variations in topographic metrics over different climates seen in other studies (Langbein and Schumm, 1958; Walling and Webb, 1983) in steady-state landscapes with homogeneous erosion rates. Comparison of simulations with homogeneous precipitation and changing values of vegetation cover (Fig. 7a,b,c) to simulations with both changing precipitation and vegetation cover (Fig. 7d,e,f) we see that we are only able to reproduce a similar trend with a distinct peak in topographic metrics when both variable precipitation and vegetation cover are considered. From this, we conclude that modern model-based landscape evolution studies that aim to compare areas with different climates should incorporate vegetation dynamics in their simulations. Misfits between the predicted and Chilean observed topographic metrics (Fig. 7d,e,f) present when the vegetation and precipitation both vary likely stem from the simplicity of the model setup used and the likelihood of differences of the rock uplift rate and lithology's present in these areas.

5.2 Interpretation of Step-Change Experiments

Our analysis shows that changes in vegetation-cover typically have a higher magnitude of impact on topographies for lower values of initial vegetation cover, compared to simulations with high initial vegetation cover (Fig. 8, 9). In those settings the influence of vegetation cover outweighs the influence of precipitation in cases of negative and positive directions of the step change. The reasons for this is due to a higher impact of changes in vegetation on erosivity and diffusivity (parameter K_v, K_d; equation 4, 8) then changes in precipitation and therefore changes in runoff have on overall erosion values.

Furthermore, a negative step change in vegetation cover impacts the topographic metrics a factor of two more than do positive step change changes (Fig. 8d,e,f). This response is interpreted to be due to the non-linear reaction of diffusivity and fluvial erodibility to changes in vegetation cover (See Fig.6). Negative changes in vegetation cover lead to a higher overall change in diffusivity and erodibility which leads to a higher sensitivity of equations 4 and 8 to negative step-changes compared to positive step-changes.

Model results for the topographic metrics and erosion rates also indicate a difference in the adjustment times of the system until a new steady state is reached when either precipitation or vegetation cover changes (Figs. 8, 9). For simulations with positive step-changes (Fig. 8a,b,c) the adjustment time for changes in vegetation cover to reach a new equilibrium in

Earth Surf. Dynam. Discuss., https://doi.org/10.5194/esurf-2018-13
Manuscript under review for journal Earth Surf. Dynam.
Discussion started: 21 February 2018

topographic metrics or erosion rates is three times higher than the adjustment time for changes in precipitation. Simulations with a negative step-changes in vegetation cover show an adjustment time which is lower by a factor of 18 compared to negative changes in precipitation. This difference in adjustment time again is a result of the non-linear behavior of erosion parameters K_d and K_v which influence how effective a signal of increasing or decreasing erosion can travel through a river basin (Perron et al., 2012). High values of K_d and K_v are associated with lower adjustment times and are a result of negative changes in vegetation cover. The influence of changing precipitation on adjustment time behaves in a more linear fashion and therefore mostly depends on the overall magnitude of change. Therefore, positive step-changes in vegetation cover decrease K_d and K_v which leads to higher adjustment times than the corresponding changes in precipitation.

An increase and then decrease, or decrease and then increase, in predicted slope and erosion rates is observed for both the positive and negative step changes experiments (Fig. 8b,e; and Fig. 9). This non-linear response in both positive and negative step changes in precipitation and vegetation cover is also manifested in the subsequent oscillation experiments, but most clearly identifiable in the step change experiments. The explanation for this behavior is as follows. A positive step change in vegetation cover (Fig. 8b) leads to a decrease in fluvial capacity because increased vegetation cover increases the Manning's roughness (parameter n_v, equation 8). The effect of changing the Manning's roughness varies with the location in the catchment and influences which processes (fluvial or hillslope) most strongly influence slopes and erosion rates. In the upper part of catchments where contributing areas (and discharge) are low, this increase in Manning's roughness causes many areas to be below threshold conditions such that fluvial erosion is less efficient, and hillslope diffusion increases in importance's and lowers slopes. In the lower part of catchments, where contributing area and discharge are higher, changes in the Manning's roughness are not large enough to impact fluvial erosion because these areas remain at, or above, threshold conditions for erosion. With time, the lower regions of the catchments that are at or above threshold conditions propagate a wave of erosion up to the higher regions that are below threshold conditions. The propagating wave of erosion eventually leads to increase in slope angles, essential due to the response time of the fluvial network to adjust to new Manning's roughness conditions.

In contrast, a positive step change in mean annual precipitation leads to an initial increase in fluvial shear stress which initially causes headward incision of river channels and leads to wave of erosion that propagates upstream and increases channel slope values (Fig. 8b, see also e.g. Bonnet and Crave, 2003). The increase in channel slopes leads to an increase in the hillslope diffusive flux adjacent to the channels that then propagates upslope. Eventually, this increase in hillslope flux leads to a decrease in hillslope angles, and an overall reductions in mean catchment slopes after the systems reaches equilibrium.

Negative step-changes in vegetation cover or precipitation (Fig. 8e, green curves) shows the opposite behavior of the previous positive step change description. A negative step change in vegetation cover leads to an initial increase of fluvial erosion everywhere in the catchment because the Manning's roughness decreases everywhere. This catchment wide decrease in Manning's roughness leads to fluvial incision everywhere in the catchment and an increase in mean slope. However, eventually hillslope processes catch up with increased slopes near the channels and with time an overall reduction of slope occurs. Negative changes in precipitation (Fig. 8e, blue curves) lead to an initial decrease in fluvial erosion which leads to an increase in the significance of hillslope processes such that slope angles between channel and ridge decrease as hillslope processes fill in channels. With time, the fluvial network equilibrates to lower precipitation conditions by increasing slopes maintain equilibrium between erosion and rock uplift rates.

Earth Surf. Dynam. Discuss., https://doi.org/10.5194/esurf-2018-13
Manuscript under review for journal Earth Surf. Dynam.
Discussion started: 21 February 2018

Thus, the contrasting behavior of either initially increasing or decreasing slopes and erosion rates, followed by a change in the opposite direction of this initial change highlight a complicated vegetation-climate induced response to changes in either parameter. This non-linear behavior, and the timescales over which these changes occur, suggest that modern-systems that experienced past changes in climate and vegetation will likely be in a state of transience and the concept of a dynamic equilibrium in hillslope angles and erosion rates may be difficult to achieve in these natural systems.

Previous studies have inferred relationships between mean catchment erosion rates derived from cosmogenic radionuclides and topographic metrics (e.g., DiBiase et al., 2010; DiBiase and Whipple, 2011). However, the previous discussion of how topographic metrics change in response to variable precipitation and vegetation suggest that empirical relationships between erosion rates and topographic metrics contain a signal of climate and vegetation cover in the catchment. We illustrate the effect of step changes in climate and vegetation on the new steady-state of topographic metrics in Figure 14. In this example, the new steady state conditions in basin relief and mean slope after a modest (+/-10%) change in vegetation or precipitation (triangles) differ from the initial steady-state condition (circles). These changes in topographic metrics when the new steady-state is achieved occur despite the rock uplift rate remaining constant. Thus, differences in mean slope and relief can occur solely due to changes in climate or vegetation and are not necessarily linked to variations in erosion rate. The change in relief or slope is most pronounced for catchments with initially low (e.g. 10%) vegetation cover.

5.3 Interpretation of Oscillation Experiments

The results from the 100kyr oscillating vegetation and precipitation conditions shows that oscillating vegetation cover without the corresponding oscillations in precipitation leads to adjustments of topographic features, to a new dynamic equilibrium after approximately 1.5Ma (Figs. 10, 11). The results indicate that the magnitude of adjustment depends on the initial vegetation cover, whereby simulations with 10% initial vegetation cover (solid lines, Fig. 10) show the largest changes from the initial (pre-oscillation) conditions to the new dynamic steady-state. Simulations with 70% initial vegetation cover (dashed lines, Fig. 10) show only minor adjustment to a new dynamic steady-state and lower amplitudes of oscillation. This is also represented by the mean basin erosion rates which show a significant peak for the first period of oscillating vegetation cover with erosion rates being 16 times higher than steady-state erosion rates for simulations with 10% initial vegetation cover whereas the peak erosion rate for 70% vegetation cover simulations is only higher by a factor of 1.4 in the first period of oscillation. The previously described response of topographic metrics and erosion rates to oscillating vegetation are due to processes described in the previous step change experiments. For example, the asymmetric oscillations in topographic metrics for V=10% (Fig. 10) are due to the superposition of positive, then negative changes described in section 5.2. Variations in the imposed Manning's roughness, and relative strengths of fluvial vs hillslope processes in different parts of the catchments at different times causes the topographic metrics and erosion rates to have a variable amplitude and shape of response from the symmetric oscillations imposed on the topography (Fig. 4a). Simulations with oscillating precipitation and constant vegetation cover however show a less pronounced shift to new equilibrium conditions and in general lower amplitudes of oscillation in both topographic metrics and erosion rate (Figs. 12, 13). This difference in the response of the topographic metrics and erosion rates in Figures 12 and 13, compared to the oscillating vegetation cover experiments (Figs 10, 11) is due to a generally higher impact of changes in vegetation cover on parameters which guide erosion rates and therefore adjustment to topographic metrics, compared to the calibrated, corresponding changes in precipitation in our model domains. Especially for simulations with low initial vegetation cover the effect of changing vegetation shows larger magnitude effects because of the non-linear response of diffusivity and fluvial erodibility to changes in vegetation cover compared to the linear response to changes in precipitation.

5.4 Coupled Oscillations in Both Vegetation and Precipitation

The previous sections present a sensitivity analysis of how step changes or oscillations in either vegetation cover or precipitation influence topography. Here we present a step-wise increase towards reality by investigating the topographic response to changes in both precipitation and climate at the same time. The amplitude of change prescribed for both precipitation and vegetation is based upon the present empirical relationship observed in the Chilean study areas for initial vegetation covers of 10 and 70%, and mean annual precipitations for 10 and 360mm/yr (Fig. 5). As with the previous experiments, oscillations in parameters were imposed upon steady-state topography that developed with the previous values, and a rock uplift rate of 0.2mm/yr.

Figure 15 shows the evolution of topographic metrics for simulations with combined oscillations in precipitation and vegetation. The variation in topographic metrics resembles those described for simulations with constant vegetation cover and oscillating climate by showing little to no significant adjustment towards new dynamic steady-state conditions. The amplitudes of oscillation are dampened from those of previous results because of the opposing effects of changes in precipitation and vegetation cover (e.g. compare blue and green curves in Figs. 8 and 9).

However, inspection of the predicted erosion rates (Fig. 16) for the combined oscillations indicates a significant (~0.1; -~0.15mm/yr), and highly non-linear response. The response between the 70% and 10% vegetation cover scenarios are very different such that for heavily vegetated areas (P(V=70%)) erosion rates typically increase during an oscillation, whereas for the low vegetation cover conditions (P(V=10%)) erosion rates initially show a decrease, and then an increase and decrease at a higher frequency.

To better understand this contrast in the response to combined precipitation and vegetation changes, the first cycle of the imposed oscillation is shown in Figure 17. After an oscillation starts, the 10% initial vegetation cover simulations show a decline in erosion rates with the minimum erosion rate correlated with highest values of both vegetation cover and mean annual precipitation (compare top and bottom panels). This part of the response is interpreted as resulting from the hindering effect of increased vegetation on erosion rates outweighing the impact of higher values of precipitation on erosion rates (Fig. 17). After values of vegetation cover and precipitation start to decline, erosion rates show a very rapid increase to values of ~0.3mm/yr. This increase in erosion rates is due to an increase in both K_v and K_d (Fig. 3b, equations 4, 5) which outcompetes the effect of precipitation decrease.

Following this, a sudden drop in erosion rates to 0mm/yr occurs and lasts for 3kyrs due to the onset of hyper arid conditions at minimum precipitation. After this low in erosion rates, they increase again to 0.3mm/yr as precipitation and vegetation cover increase while the effect of increased precipitation outweighs the effect of the non-linear decrease in K_v and K_d (Fig. 3b, c; equations 4, 5). Finally, at the end of this complex cycle a decrease in erosion rates occurs (Fig. 17b) while vegetation and precipitation are increasing (upper panel) because the effect of vegetation increases K_v/K_d and outweights the effect of increasing precipitation.

Lastly, a clearly different behavior in erosion rates occurs for settings with higher vegetation cover (e.g. P(V=70%)) compared to the previous lower vegetation cover scenarios. As the vegetation cover and precipitation increase (Fig. 17a) in the first half of the 100kyr cycle, the erosion rates increase to values of approximately 0.35mm/yr. This is due the increase in precipitation which outcompetes the decline in erosivity/diffusivity parameters K_d and K_v. Following this, when vegetation cover and precipitation decrease in the second half of the cycle, little to no change occurs in the erosion

Earth Surf. Dynam. Discuss., https://doi.org/10.5194/esurf-2018-13
Manuscript under review for journal Earth Surf. Dynam.
Discussion started: 21 February 2018

rates. This near static behavior in erosion rates while precipitation and vegetation cover decrease is due to an equilibrium between the negative effect on erosion rates for decreasing precipitation and the positive effect on erosion rates for decreasing vegetation cover.

In summary, the non-linear shape of the vegetation dependent erosivity (K_v) and hillslope diffusivity (K_d) in combination with linear effects of mean annual precipitation on erosion rates, exert a primary control on the direction and magnitude of change in catchment average erosion rates. Despite a simple oscillating behavior in precipitation and vegetation cover, a complex and non-linear response in erosion rates occurs. The implications of this are large for observational studies of catchment average erosion rates and suggest that the direction and magnitude of response observed in a setting is highly dependent on the mean vegetation and precipitation conditions of the catchment, as well as what time the observations are made within the cycle of the varying vegetation and precipitation. Furthermore, these results highlight the need for future modeling studies (and motivation for our ongoing work), to investigate the response of catchment topography and erosion rates to more realistic climate and vegetation change scenarios, as well as a broader range of initial vegetation covers and precipitation rates than those explored here such that the threshold in behavior between the two curves shown in figure 17b can be understood.

This could be achieved by using simulation results from state-of-art dynamic vegetation models (e.g Smith et al., 2014; see also companion paper by Werner et al., 2018) as inputs into the landscape evolution model or by full coupling between both model types. Vegetation simulations could, e.g. benefit from simulated changes in soil depth, which can crucially determine plant water stress, provided by the landscape evolution model. Coupling between Landlab and the dynamic regional to global vegetation model LPJ-GUESS (Smith et al., 2014; Werner et al., 2018) is envisioned.

5.5 Model Restrictions and Caveats

Like other previous work on this topic (Collins et al., 2004; Istanbulluoglu and Bras 2005) the model setup used in this study was intentionally simplified to document how different vegetation and climate related factors impact topography over long (geologically relevant) timescales. We acknowledge that future model-studies should address some of the restrictions imposed by our approach to evaluate their significance for the results presented here. Future work should consider a transport-limited fluvial model or a fully-coupled alluvial sedimentation and transport model. Addition of this could bring new understanding in to how vegetation not only influences detachment limited systems, but also influences sedimentation and entrainment of material. This added level of complexity could however limit (due to computational concerns) the temporal scales over the investigation can be conducted. Future studies could improve upon this work by considering a more in-depth parameterization of how vegetation related processes (e.g. root depth and density, plant functional type) influence topographic metrics and erosion rates. Due to the long-timescales considered here, mean annual precipitation rather than a stochastic distribution of precipitation was implemented. Future work should evaluate how stochastic distributions in precipitation and extreme events in arid, poorly vegetation settings, impact these results.

Regarding the vegetation and water-budget, a more sophisticated model of evapotranspiration and infiltration as a function to surface plant cover and plant functional traits such as rooting depth would improve model predictions and is a priority goal of future research within this project. Improvements will come from planned coupling of surface process model with the dynamic vegetation model LPJ-GUESS (Werner et al., 2018, this issue).

We also acknowledge here that the transient forcings we have chosen for driving our model are simplistic and could be improved by a higher-fidelity time-series of climate over the last millennia. We choose a 100kyr, eccentricity driven, periodicity because it is widely recognized that the eccentricity cycles are a main control in driving Earths glacial cycle over the last 0.9Ma. While this approach is reasonable for a sensitivity analysis such as we've conducted, it prohibits a detailed comparison to observations without additional refinement. Our results suggest that a shorter periodicity, which would resemble other periodicities in the Milankovitch cycle (e.g., 41kyrs, 23kyrs) or shorter time scale climate variations, such as Heinrich events (see Huntley et al., 2013) would lead to smaller magnitudes of adjustment to new dynamic equilibria, because of short timespans in high-/low-erosive climate conditions within one period.

6. Conclusions

The results from our model-based experiments in comparison to observations from topographic analysis from four different areas in the Coastal Cordillera in Chile show that the interactions of vegetation cover and mean annual precipitation on the evolution of landscapes is a complex system with competing effects. Main conclusion which emerge from this study are:

(I) vegetation cover in general has a hindering effect on eroding surface processes but the magnitude on which changes in vegetation cover affect these processes is a function of the initial state of the system. Changes in systems with higher initial values of vegetation cover have a less pronounced effect than changes in systems with lower initial vegetation cover.

(II) In comparison to the Coastal Cordilleras of Chile, the relationship between precipitation and surface vegetation cover shows a distinct shape: For a 10% increase in surface vegetation cover, the corresponding increase in mean annual precipitation is smaller in areas of lower vegetation cover and increases for areas with higher vegetation cover. This has an effect on transient topographies by shifting the equilibrium of vegetation and precipitation effects on erosion rates.

(III) Following our step-change simulations, our model results show different behaviors for changes in vegetation-cover and mean annual precipitation. While increases in mean annual precipitation have an increasing effect on erosion rates and therefore a long-term negative effect on topographic metrics, an increase in vegetation cover hinders erosion, and leads to higher topographic metrics. The magnitude of these changes is highly dependent on the initial vegetation cover and precipitation before the step-change.

(IV) Simulations with either oscillating vegetation cover or oscillating precipitation show adjustments to new dynamic mean values around which the basin metrics oscillate. The magnitude of adjustment is highly sensitive to initial vegetation cover, where simulations with 10% initial cover show higher magnitudes than simulations with 70% cover, for oscillating vegetation. Oscillating precipitation leads to lower-/no adjustments but an oscillation of basin metrics around the initial mean values with generally lower amplitudes compared to simulations with oscillating vegetation cover.

(V) Simulations with coupled oscillations of both vegetation cover and precipitation show only small magnitudes of adjustments of topography metrics to new dynamic equilibriums similar to simulations with a oscillation in only precipitation. However corresponding erosion rates show a complex pattern of rapid increases and decreases which results from a interplay of competing effects of hindering of erosion by vegetation and aiding of erosion by precipitation.

Taken together, the above findings from this study highlight a non-linear and highly variable behavior in how variations in vegetation cover impact erosion and topographic properties. The complexity in how vegetation cover and precipitation changes influence topography highlights the need for future work to consider both of these factors in tandem, rather singling out either parameter (vegetation cover or precipitation) to understand potential transients in topography.

Acknowledgements:

This study was funded as part of the German science foundation priority research program EarthShape: Earth surface shaping by biota (grant EH329-14-1 to T.A.E. and T.H.). We thank XXX and YYY for constructive reviews that improved the manuscript. We thank the national park service in Chile (CONAF) for providing access to, and guidance through, the study areas during field trips. Daniel Hobley and the LandLab 'slack' community are thanked for constructive suggestions during the Landlab program modifications implemented for this study.

References

Acosta, V. T., Schildgen, T. F., Clarke, B. A., Scherler, D., Bookhagen, B., Wittmann, H., von Blanckenburg, F. and Strecker, M. R.: Effect of vegetation cover on millennial-scale landscape denudation rates in East Africa, Lithosphere, 7(4), 408–420, doi:10.1130/L402.1, 2015.

Allen, C. D. and Breshears, D. D.: Drought-induced shift of a forest–woodland ecotone: rapid landscape response to climate variation, Proceedings of the National Academy of Sciences, 95(25), 14839–14842, 1998.

Allen, C. D., Macalady, A. K., Chenchouni, H., Bachelet, D., McDowell, N., Vennetier, M., Kitzberger, T., Rigling, A., Breshears, D. D., Hogg, E. H. (Ted), Gonzalez, P., Fensham, R., Zhang, Z., Castro, J., Demidova, N., Lim, J.-H., Allard, G., Running, S. W., Semerci, A. and Cobb, N.: A global overview of drought and heat-induced tree mortality reveals emerging climate change risks for forests, Forest Ecology and Management, 259(4), 660–684, doi:10.1016/j.foreco.2009.09.001, 2010.

Amundson, R., Heimsath, A., Owen, J., Yoo, K. and Dietrich, W. E.: Hillslope soils and vegetation, Geomorphology, 234, 122–132, doi:10.1016/j.geomorph.2014.12.031, 2015.

Andriessen, P. A. and Reutter, K.-J.: K-Ar and fission track mineral age determination of igneous rocks related to multiple magmatic arc systems along the 23 S latitude of Chile and NW Argentina, Tectonics of the southern central Andes: structure and evolution of an active continental margin, 141–154, 1994.

Avdievitch, N. N., Ehlers, T. A. and Glotzbach, C.: Slow long-term exhumation of the West Central Andean Plate Boundary, Tectonics, 2017.

Bachelet, D., Neilson, R. P., Hickler, T., Drapek, R. J., Lenihan, J. M., Sykes, M. T., Smith, B., Sitch, S. and Thonicke, K.: Simulating past and future dynamics of natural ecosystems in the United States, Global Biogeochemical Cycles, 17(2), doi:10.1029/2001GB001508, 2003.

Blois, J. L., Williams, J. W., Fitzpatrick, M. C., Jackson, S. T. and Ferrier, S.: Space can substitute for time in predicting climate-change effects on biodiversity, Proceedings of the National Academy of Sciences, 110(23), 9374–9379, 2013.

Bonnet, S. and Crave, A.: Landscape response to climate change: Insights from experimental modeling and implications for tectonic versus climatic uplift of topography, Geology, 31(2), 123–126, 2003.

Broxton, P. D., Zeng, X., Scheftic, W. and Troch, P. A.: A MODIS-Based Global 1-km Maximum Green Vegetation Fraction Dataset, Journal of Applied Meteorology and Climatology, 53(8), 1996–2004, doi:10.1175/JAMC-D-13-0356.1, 2014.

Carretier, S., Regard, V., Vassallo, R., Aguilar, G., Martinod, J., Riquelme, R., Pepin, E., Charrier, R., Herail, G., Farias, M., Guyot, J.-L., Vargas, G. and Lagane, C.: Slope and climate variability control of erosion in the Andes of central Chile, Geology, 41(2), 195–198, doi:10.1130/G33735.1, 2013.

Collins, B. D., Bras, R. L. and Tucker, G. E.: Modeling the effects of vegetation-erosion coupling on landscape evolution, Journal of Geophysical Research, 109(F3), doi:10.1029/2003JF000028, 2004.

Culling, W. E. .: Analytical Theory of Erosion, The Journal of Geology, 68(3), 336–344, 1960.

Curran, J. C. and Hession, W. C.: Vegetative impacts on hydraulics and sediment processes across the fluvial system, Journal of Hydrology, 505, 364–376, doi:10.1016/j.jhydrol.2013.10.013, 2013.

DiBiase, R. A. and Whipple, K. X.: The influence of erosion thresholds and runoff variability on the relationships among topography, climate, and erosion rate, Journal of Geophysical Research, 116(F4), doi:10.1029/2011JF002095, 2011.

DiBiase, R. A., Whipple, K. X., Heimsath, A. M. and Ouimet, W. B.: Landscape form and millennial erosion rates in the San Gabriel Mountains, CA, Earth and Planetary Science Letters, 289(1–2), 134–144, doi:10.1016/j.epsl.2009.10.036, 2010.

Dosseto, A., Hesse, P. P., Maher, K., Fryirs, K. and Turner, S.: Climatic and vegetation control on sediment dynamics during the last glacial cycle, Geology, 38(5), 395–398, doi:10.1130/G30708.1, 2010.

Feng, X., Wang, Y., Chen, L., Fu, B. and Bai, G.: Modeling soil erosion and its response to land-use change in hilly catchments of the Chinese Loess Plateau, Geomorphology, 118(3–4), 239–248, doi:10.1016/j.geomorph.2010.01.004, 2010.

Fernandez, N. F. and Dietrich, W.: Hillslope evolution by diffusive processes: The timescale for equilibrium adjustments, Water Resources Research, 33(6), 1307–1318, 1997.

Gilbert, G. K.: Report on the Geology of the Henry Mountains, Dept of the Interior, US Govt Printing Office, Washington, DC., 1877.

Gyssels, G., Poesen, J., Bochet, E. and Li, Y.: Impact of plant roots on the resistance of soils to erosion by water: a review, Progress in Physical Geography, 29(2), 189–217, doi:10.1191/0309133305pp443ra, 2005.

Hobley, D. E. J., Adams, J. M., Nudurupati, S. S., Hutton, E. W. H., Gasparini, N. M., Istanbulluoglu, E. and Tucker, G. E.: Creative computing with Landlab: an open-source toolkit for building, coupling, and exploring two-dimensional numerical models of Earth-surface dynamics, Earth Surface Dynamics, 5(1), 21–46, doi:10.5194/esurf-5-21-2017, 2017.

Howard, A. D. and Kerby, G.: Channel changes in badlands, Geological Society of America Bulletin, 94(6), 739–752, 1983.

Hughes, L.: Biological consequences of global warming: is the signal already, TREE, 15(2), 2000.

Huntley, B., Allen, J. R. M., Collingham, Y. C., Hickler, T., Lister, A. M., Singarayer, J., Stuart, A. J., Sykes, M. T. and Valdes, P. J.: Millennial Climatic Fluctuations Are Key to the Structure of Last Glacial Ecosystems, edited by J. Mohan, PLoS ONE, doi:10.1371/journal.pone.0061963, 2013.

Istanbulluoglu, E. and Bras, R.: Vegetation-modulated landscape evolution: Effects of vegetation on landscape processes, drainage density, and topography, Journal of Geophysical Research, 110(F2), doi:10.1029/2004JF000249, 2005.

Istanbulluoglu, E., Tarboton, D. G., Pack, R. T. and Luce, C. H.: Modeling of the interactions between forest vegetation, disturbances, and sediment yields, Journal of Geophysical Research: Earth Surface, 109(F1) doi:10.1029/2003JF000041, 2004.

Jeffery, M. L., Yanites, B. J., Poulsen, C. J. and Ehlers, T. A.: Vegetation-precipitation controls on Central Andean topography, Journal of Geophysical Research: Earth Surface, 119(6), 1354–1375, doi:10.1002/2013JF002919, 2014.

Juez-Larré, J., Kukowski, N., Dunai, T. J., Hartley, A. J. and Andriessen, P. A. M.: Thermal and exhumation history of the Coastal Cordillera arc of northern Chile revealed by thermochronological dating, Tectonophysics, 495(1–2), 48–66, doi:10.1016/j.tecto.2010.06.018, 2010.

Langbein, W. B. and Schumm, S. A.: Yield of sediment in relation to mean annual precipitation, Eos, Transactions American Geophysical Union, 1958.

Ledru, M.-P., Labouriau, M. L. S. and Lorscheitter, M. L.: Vegetation dynamics in southern and central Brazil during the last 10,000 yr B.P., Review of Palaeobotany and Palynology, 99, 131–142, 1997.

Maksaev, V. and Zentilli, M.: Fission Track Thermochronology of the Domeyko Cordillera, Northern Chile: Implications for Andean Tectonics and Porphyry Copper Metallogenesis, Exploration and Mining Geology, 8, 65–89, 2000.

Marston, R. A.: Geomorphology and vegetation on hillslopes: Interactions, dependencies, and feedback loops, Geomorphology, 116(3–4), 206–217, doi:10.1016/j.geomorph.2009.09.028, 2010.

McInnes, B. I. A., Farley, K. A., Sillitoe, R. and Kohn, B. P.: Application of Apatite (U-th)/He Thermochronometry to the determination of the sense and amount of vertical fault displacement at the Chuquicamata Porphyry Copper Deposit, Chile, Economic Geology, 94, 937–948, 1999.

McPhillips, D., Bierman, P. R., Crocker, T. and Rood, D. H.: Landscape response to Pleistocene-Holocene precipitation change in the Western Cordillera, Peru: 10Be concentrations in modern sediments and terrace fills, J. Geophys. Res. Earth Surf., 118(4), 2013JF002837, doi:10.1002/2013JF002837, 2013.

Muhs, D. R., T. A. Ager and Beget, J. E.: Vegetation and paleoclimate of the last interglacial period, central Alaska, Quaternary Science Reviews, 20, 41–61, 2001.

Perron, J. T., Richardson, P. W., Ferrier, K. L. and Lapôtre, M.: The root of branching river networks, Nature, 492(7427), 100–103, doi:10.1038/nature11672, 2012.

Prentice, I. C., Harrison, S. P. and Bartlein, P. J.: Global vegetation and terrestrial carbon cycle changes after the last ice age, New Phytologist, 189(4), 988–998, doi:10.1111/j.1469-8137.2010.03620.x, 2011.

Reinhardt, L., Jerolmack, D., Cardinale, B. J., Vanacker, V. and Wright, J.: Dynamic interactions of life and its landscape: feedbacks at the interface of geomorphology and ecology, Earth Surface Processes and Landforms, 35(1), 78–101, doi:10.1002/esp.1912, 2010.

Roering, J. J., Almond, P., Tonkin, P. and McKean, J.: Soil transport driven by biological processes over millennial time scales, Geology, 30(12), 1115–1118, 2002.

Sangireddy, H., Carothers, R. A., Stark, C. P. and Passalacqua, P.: Controls of climate, topography, vegetation, and lithology on drainage density extracted from high resolution topography data, Journal of Hydrology, 537, 271–282, doi:10.1016/j.jhydrol.2016.02.051, 2016.

Schaller, M., von Blanckenburg, F., Veldkamp, A., Tebbens, L. A., Hovius, N. and Kubik, P. W.: A 30 000 yr record of erosion rates from cosmogenic 10Be in Middle European river terraces, Earth and Planetary Science Letters, 204(1–2), 307–320, doi:10.1016/S0012-821X(02)00951-2, 2002.

Smith, B., Wårlind, D., Arneth, A., Hickler, T., Leadley, P., Siltberg, J. and Zaehle, S.: Implications of incorporating N cycling and N limitations on primary production in an individual-based dynamic vegetation model, Biogeosciences, 11(7), 2027–2054, doi:10.5194/bg-11-2027-2014, 2014.

Stephan, U. and Gutknecht, D.: Hydraulic resistance of submerged flexible vegetation, Journal of Hydrology, 269(1), 27–43, 2002.

Tucker, G., Lancaster, S., Gasparini, N. and Bras, R.: The channel-hillslope integrated landscape development model (CHILD), in Landscape erosion and evolution modeling, pp. 349–388, Springer., 2001.

Tucker, G. E. and Hancock, G. R.: Modelling landscape evolution, Earth Surface Processes and Landforms, 35(1), 28–50, doi:10.1002/esp.1952, 2010.

Vergani, C., Giadrossich, F., Buckley, P., Conedera, M., Pividori, M., Salbitano, F., Rauch, H., Lovreglio, R. and Schwarz, M.: Root reinforcement dynamics of European coppice woodlands and their effect on shallow landslides: A review, Earth-Science Reviews, 167, 88–102, doi:10.1016/j.earscirev.2017.02.002, 2017.

Walling, D. and Webb, B.: Patterns of sediment yield, Background to Palaehydrology, 69–100, 1983.

Walther, G.-R., Post, E., Convey, P., Menzel, A., Parmesan, C., Beebee, T. J., Fromentin, J.-M., Hoegh-Guldberg, O. and Bairlein, F.: Ecological responses to recent climate change, Nature, 416(6879), 389–395, 2002.

Werner, C., Schmid, M., Ehlers, T. A., Fuentes-Espoz, J. P., Steinkamp, J., Forrest, M., Liakka, J. and Hickler, T.: Effect of changing vegetation on denudation (part 1): Predicted vegetation composition and cover over the last 21 thousand years, Earth Surface Dynamics, submitted

Whipple, K. X. and Tucker, G. E.: Dynamics of the stream-power river incision model: Implications for height limits of mountain ranges, landscape response timescales, and research needs, J. Geophys. Res., 104(B8), 17661–17674, doi:10.1029/1999JB900120, 1999.

Willgoose, G., Bras, R. L. and Rodriguez-Iturbe, I.: Results from a new model of river basin evolution, Earth Surface Processes and Landforms, 16(3), 237–254, 1991.

Zachos, J., Pagani, M., Sloan, L., Thomas, E. and Billups, K.: Trends, Rhythms, and Aberrations in Global Climate 65 Ma to Present, Science, 292(5517), 686–693, doi:10.1126/science.1059412, 2001.

Zhou, Z. C., Shangguan, Z. P. and Zhao, D.: Modeling vegetation coverage and soil erosion in the Loess Plateau Area of China, Ecological Modelling, 198(1–2), 263–268, doi:10.1016/j.ecolmodel.2006.04.019, 2006.

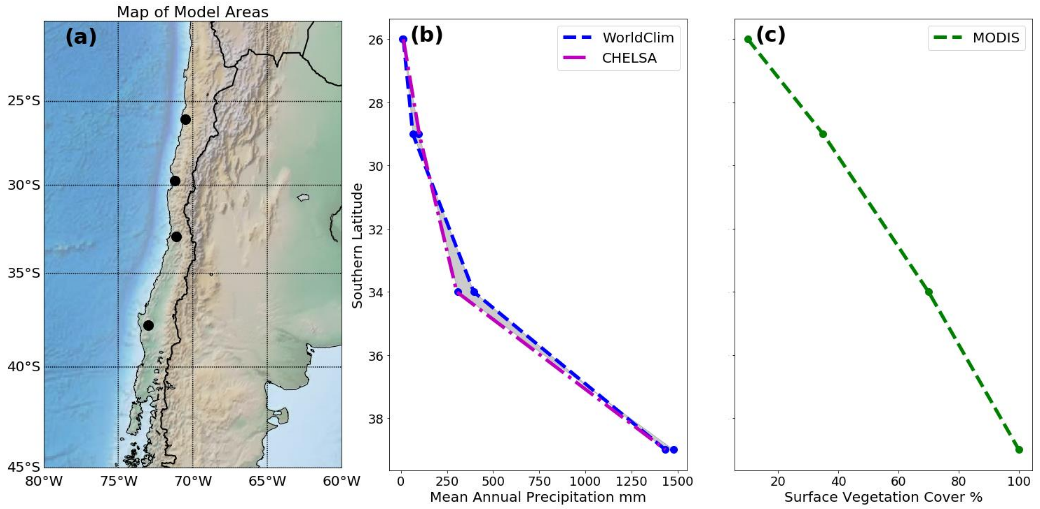

Figure 1 Overview of the geographic location, precipitation, and vegetation cover of the Coastal Cordillera, Chile studies areas used for model setup up. A) Digital topography of the areas considered and corresponding to the EarthShape (www.earthshape.net) focus areas where ongoing related research is located. B) Observed present day mean annual precipitation from the WorldClim and CHELSA datasets used as model input. B) Present day maximum surface vegetation cover from MODIS data.

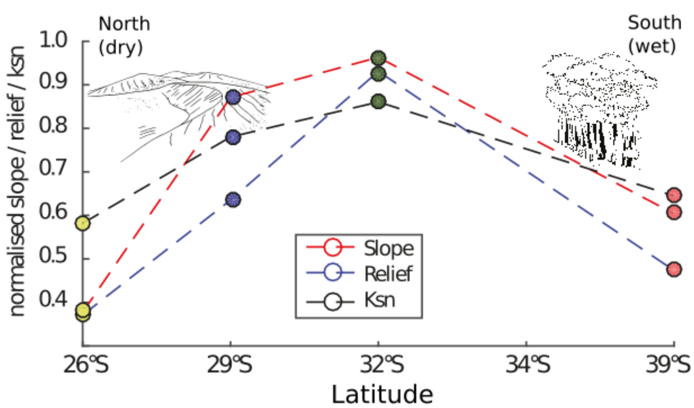

Figure 2 Normalized basin metrics for study-areas derived from 90 m SRTM digital topography from the study areas shown in Figure 1a Dots represent cumulative mean values calculated for all locations using 5-8 representative catchments in each area. Dotted lines represent linear interpolation for normalized slope, relief and channel steepness (k_{sn}) values. Note the gradual increase, then decrease in all metrics around study area at ~32°S.

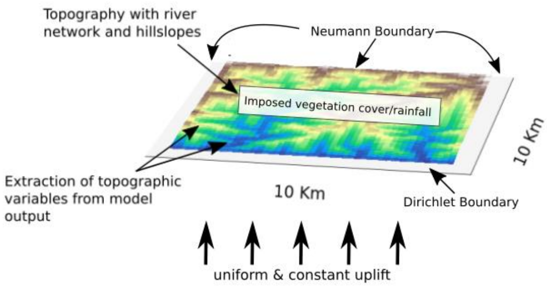

Figure 3 Example model setup used in simulations in this study. Boundary conditions and parameterizations used in the models are labeled. Blue colors represent low elevations, brown colors represent higher elevations. Additional details of parameters used are specified in Table 1.

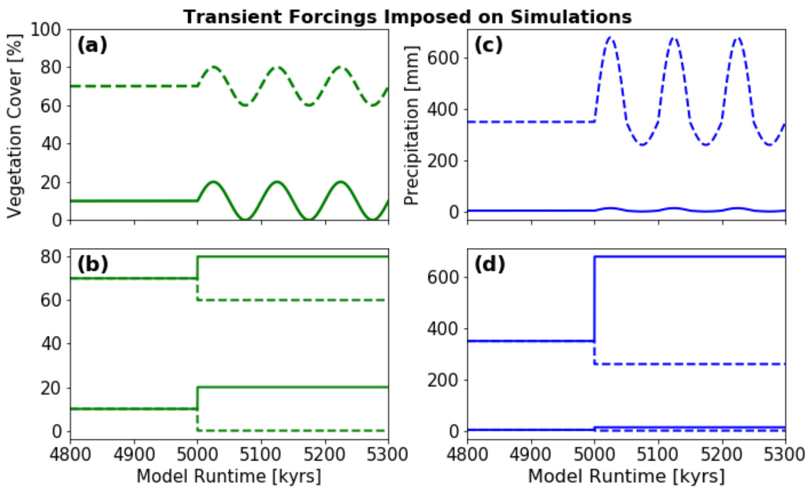

Figure 4 Transient forcings in vegetation (a,b) and precipitation (c,d) considered in model experiments. Simulations were run for 15 Myr prior to the runtime show in the figure. All transients imposed started a runtime of 5 Myr. A) Variations in vegetation cover imposed in the oscillating experiment conditions for initial vegetation cover of 10 and 70%. B) Positive and negative step change parameterizations for vegetation cover. C) Variations in mean oscillating annual precipitation. D) Positive and negative step changes in mean annual precipitation used in experiments. The initial precipitation amounts prior to the transient oscillations or step changes correspond to the observed precipitation corresponding to the vegetation cover in each of the observed study areas (Fig. 1). See also Figure 5.

Earth Surf. Dynam. Discuss., https://doi.org/10.5194/esurf-2018-13
Manuscript under review for journal Earth Surf. Dynam.
Discussion started: 21 February 2018

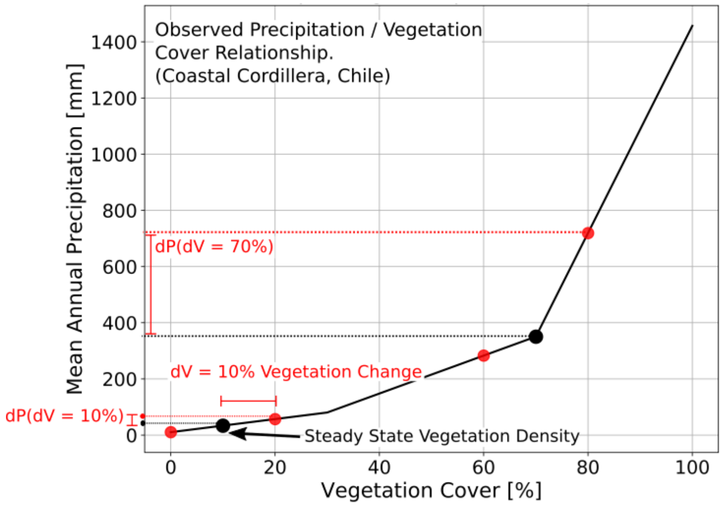

Figure 5 Graphical representation of the observed precipitation – vegetation relationship in the focus areas (Fig. 1) and how precipitation amounts were selected when perturbations in vegetation cover were imposed. Black dots represent vegetation-precipitation values used in the steady-state model conditions and prior to any transients. Red dots show how vegetation cover perturbations in +/- 10% in the model simulations were used to select corresponding mean annual precipitation amounts.

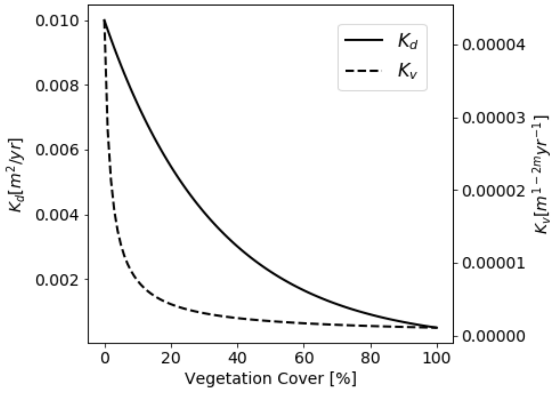

Figure 6 Predicted values of hillslope diffusivity K_d (solid line) and fluvial erodibility K_v (dashed line) as a function of vegetation surface cover. Although absolute values can't be compared due to different units, the shape of the curves representing the different parameters show different sensitivities to changes in vegetation cover. Fluvial erodibility shows highest magnitude of change for vegetation cover values < 25% whereas hillslope diffusivity reacts in a more linearly with highest change below < 65% vegetation cover.

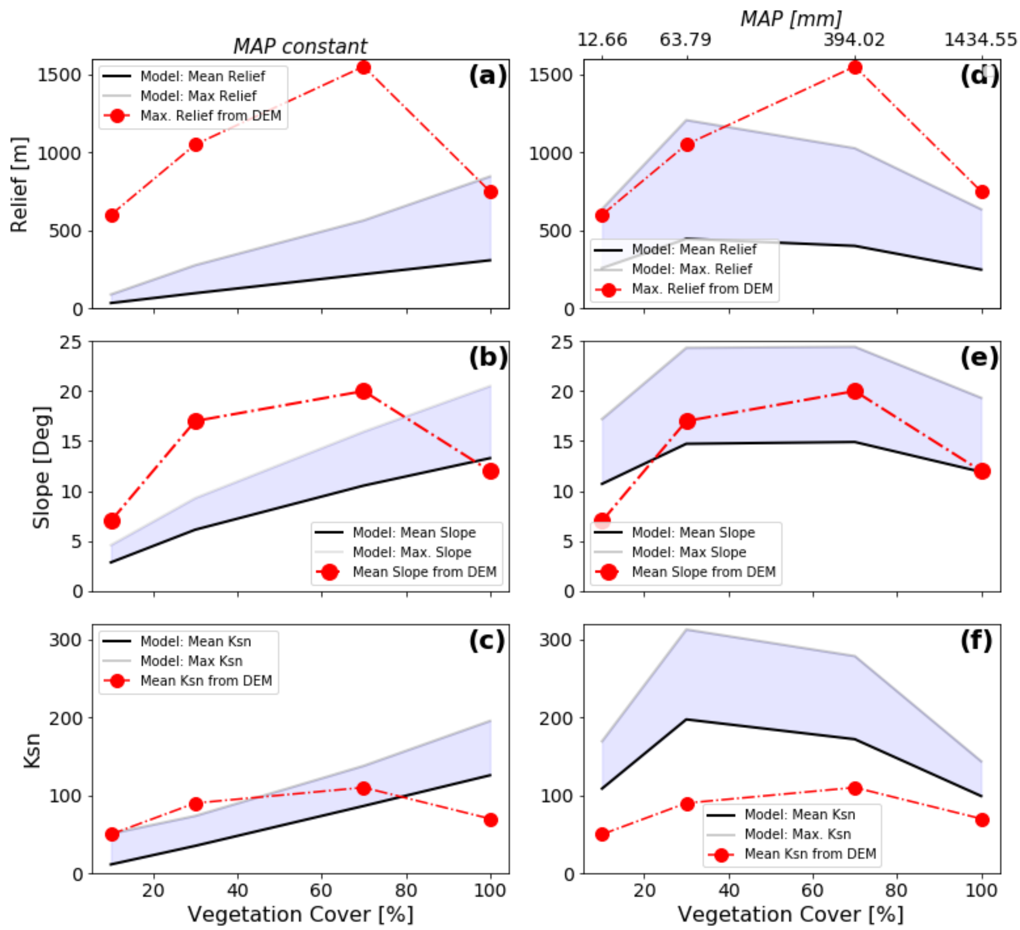

Figure 7 Steady-state model predicted (shaded regions) and observed (red dots) topographic metrics from the study areas shown in Figure 1 for different vegetation cover amounts. Observed topographic metrics were extracted from SRTM 90 m DEM. Model predicted values are shown for the cases of constant mean annual precipitation (a,b,c) or variable precipitation (D,E,F). Variable precipitation rates and vegetation covers were selected for these simulations using the observed values from the focus areas (Fig. 5). Note that for variable precipitation and vegetation cover simulations (d,e,f) the predicted values (similar to the observations) develop a humped shape pattern of an increase and then decrease in each parameter suggesting the changes in both precipitation and vegetation cover are needed to reproduce the general trend seen in observations. The sources of misfit between the predicted and observed values are due to the simplified (and untuned) setup of the simulations and discussed in the text.

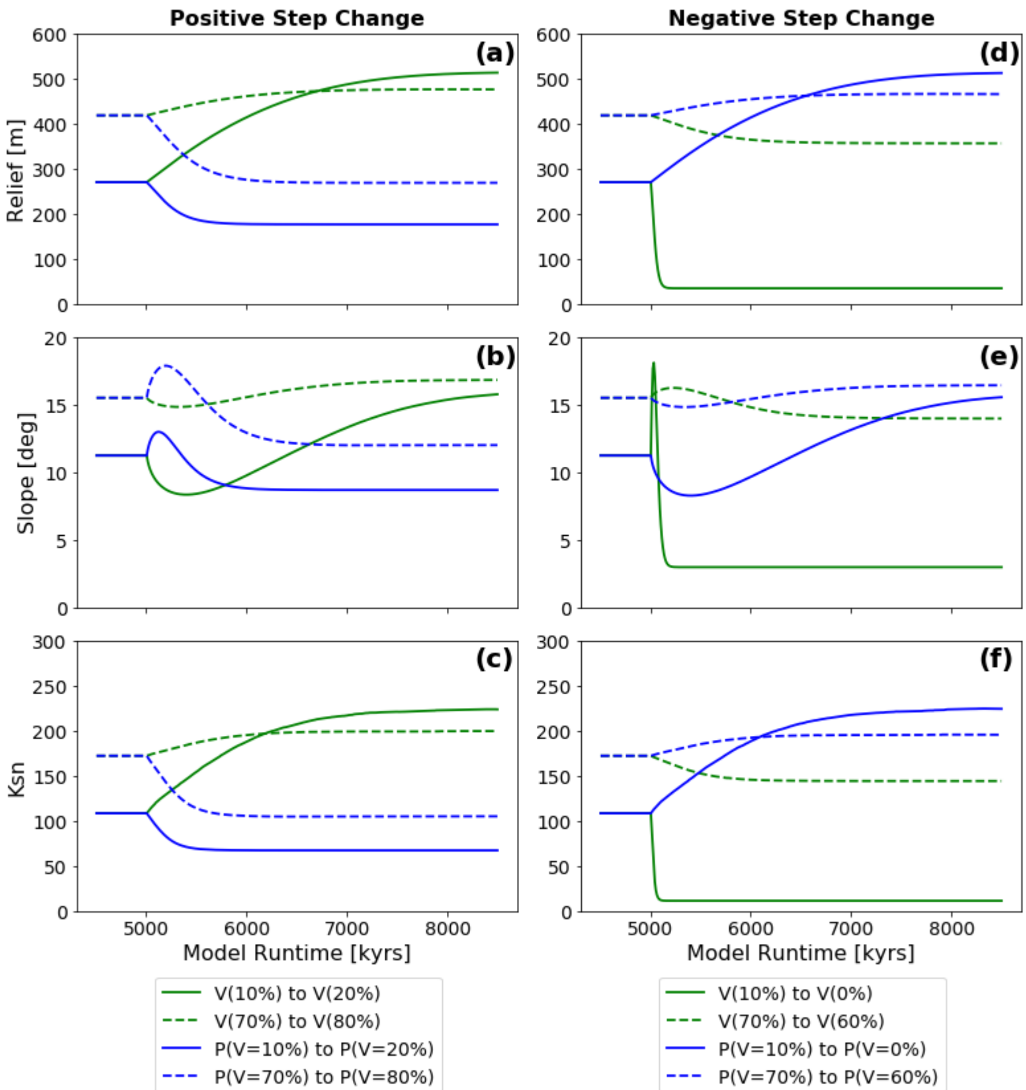

Figure 8 Observed evolution of topographic metrics after a step-change in either vegetation (green lines) or mean annual precipitation (blue lines). Results are shown for two different initial vegetation cover amounts of V=10 and 70%. Imposed mean annual precipitation changes were done by selecting the precipitation amount corresponding to the initial and final vegetation amounts used in the simulations for vegetation cover 'only' change. Panels a,b,c show reaction of model topographies to positive changes in boundary conditions, panels d,e,f show reaction to negative changes in boundary conditions.

Earth Surf. Dynam. Discuss., https://doi.org/10.5194/esurf-2018-13
Manuscript under review for journal Earth Surf. Dynam.
Discussion started: 21 February 2018

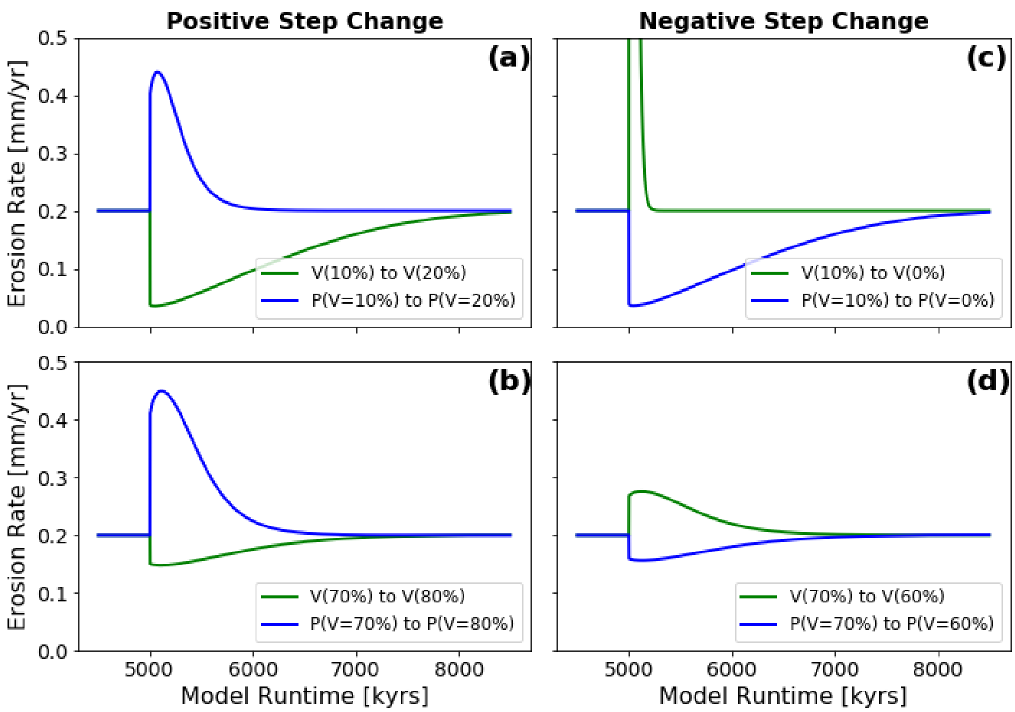

Figure 9 Mean catchment-wide erosion rates after step-change disturbance in model boundary conditions. Blue lines represent erosion rates for models with changes in only precipitation, green lines represent erosion rates for models with changes in only vegetation cover. Panels a,b show evolution after positive step-change, panels c,d for models with negative step-change. Note that the direction of change (positive or negative) from the initial state is in opposite directions for precipitation and vegetation cover changes. This effect is manifested in the subsequent plots.

Earth Surf. Dynam. Discuss., https://doi.org/10.5194/esurf-2018-13
Manuscript under review for journal Earth Surf. Dynam.
Discussion started: 21 February 2018

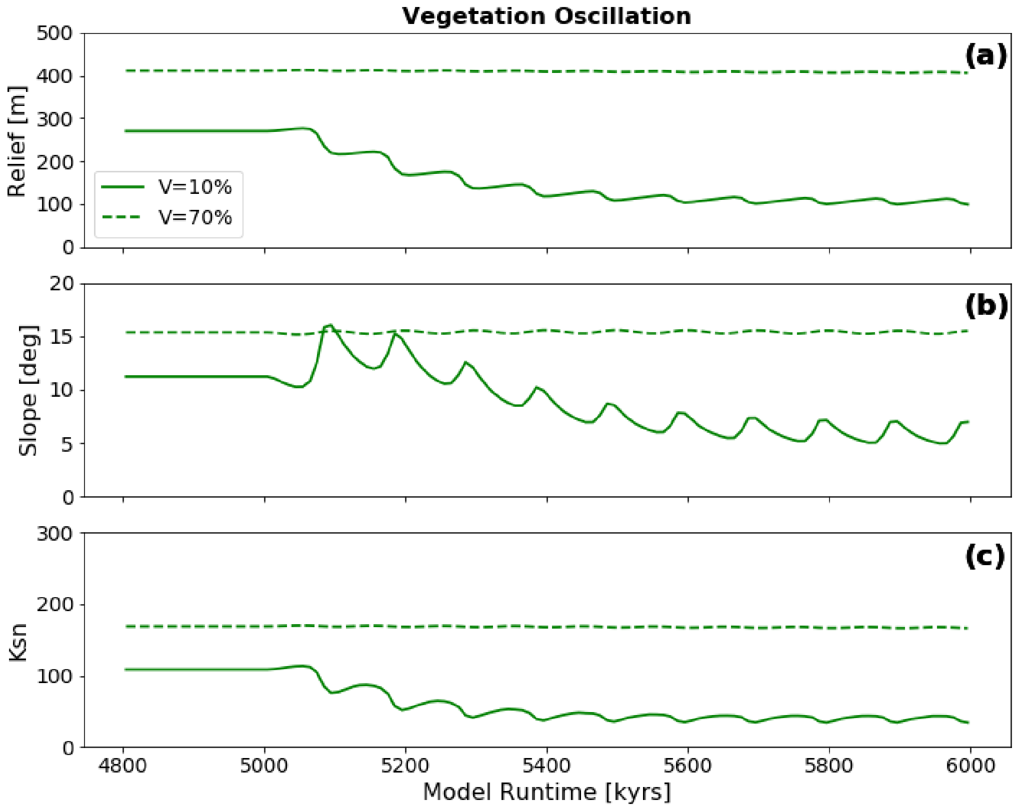

Figure 10 Evolution of topographic metrics for simulations with oscillating surface vegetation cover and constant precipitation corresponding to the initial vegetation cover prior to the transient in vegetation cover. Panels a,b,c show mean basin relief, mean basin slope and mean basin channel steepness (k_{sn}), respectively.

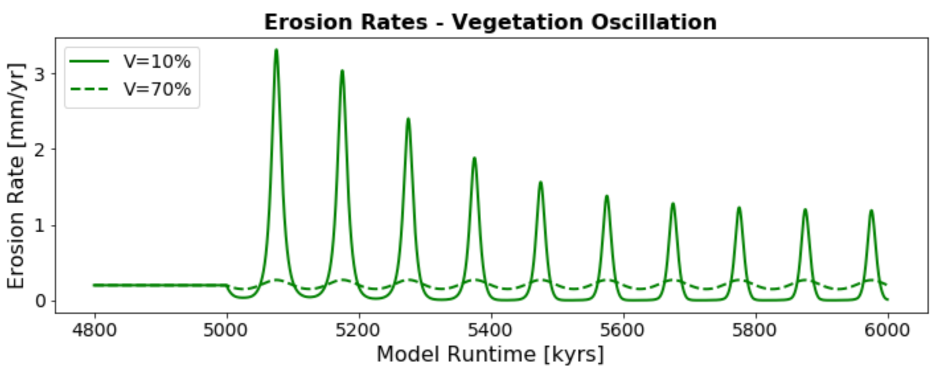

Figure 11 Predicted mean catchment erosion rates for simulations with oscillating surface vegetation cover and constant precipitation.

Earth Surf. Dynam. Discuss., https://doi.org/10.5194/esurf-2018-13
Manuscript under review for journal Earth Surf. Dynam.
Discussion started: 21 February 2018

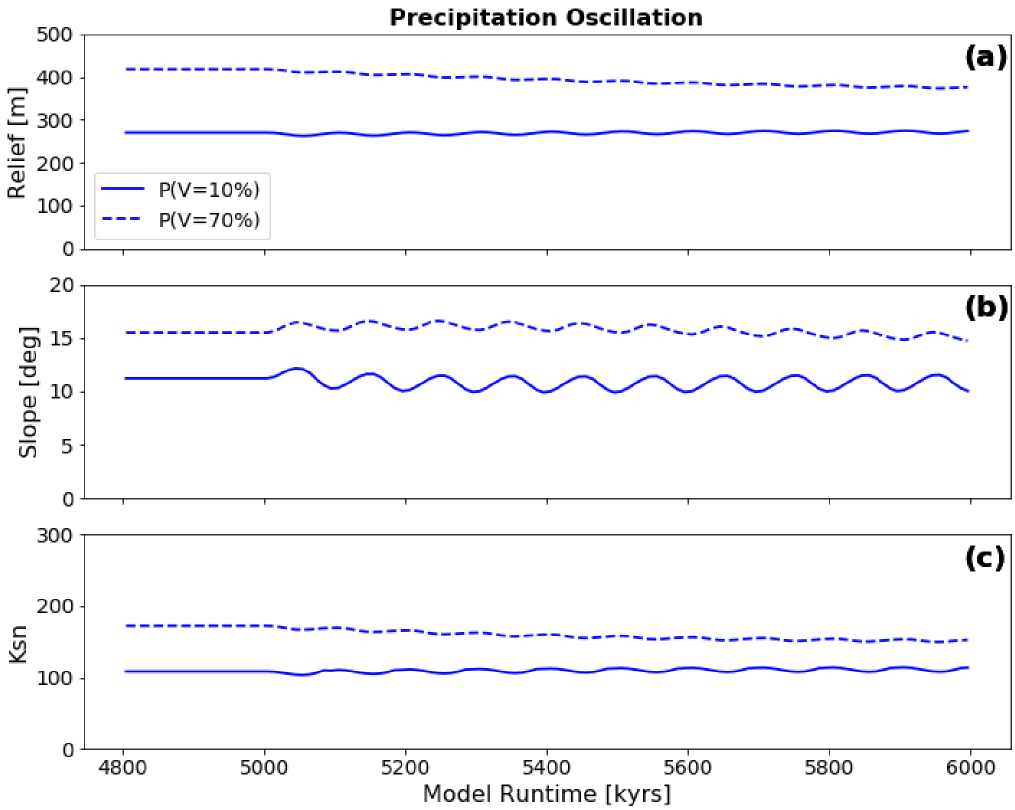

Figure 12 Evolution of topographic metrics for simulations with oscillating mean annual precipitation and constant vegetation cover. The vegetation cover was held constant at the value corresponding to the precipitation rate prior to the onset of the transient at 5000 kyrs. Panels a,b,c show mean basin relief, mean basin slope and mean basin channel steepness (k_{sn}), respectively.

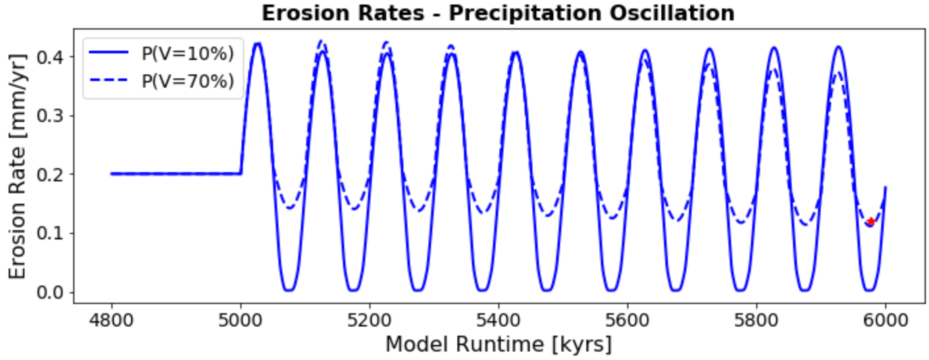

Figure 13 Mean catchment erosion rates for simulations with oscillating mean annual precipitation and constant surface vegetation cover.

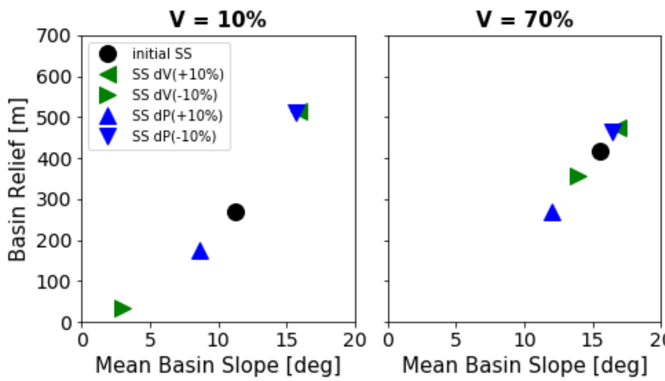

Figure 14 Shifts in mean basin slope/mean basin relief relationship for simulations with positive and negative step-changes in either vegetation cover (green triangles) or mean annual precipitation (blue triangles). Black dots represent initial steady-state conditions prior to any imposed transient in vegetation cover or mean annual precipitation.

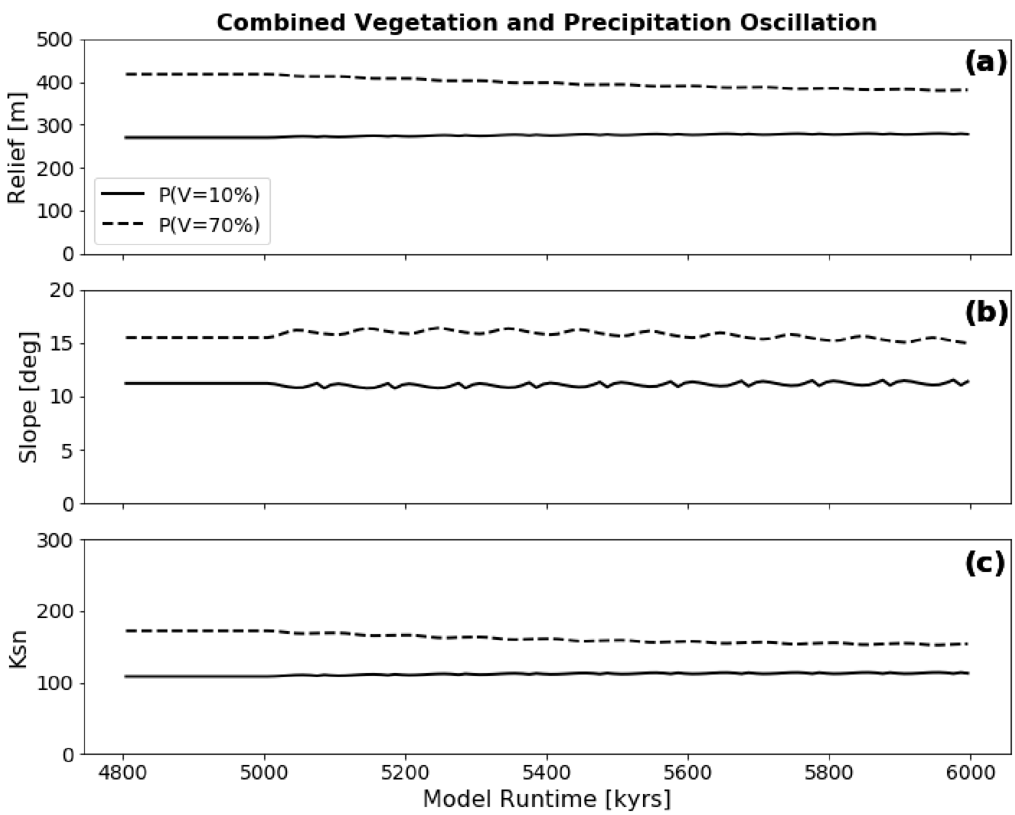

Figure 15 Evolution of topographic metrics for coupled simulations where both changes in surface vegetation cover and a corresponding change (Fig. 5) in mean annual precipitation are simultaneously imposed. Panels a,b,c show evolution of mean basin relief, mean basin slope and mean basin channel steepness (k_{sn}) after start of oscillation at 5Ma. Note the muted/damped response relative to previous simulations of oscillating vegetation cover or precipitation conditions.

Earth Surf. Dynam. Discuss., https://doi.org/10.5194/esurf-2018-13
Manuscript under review for journal Earth Surf. Dynam.
Discussion started: 21 February 2018

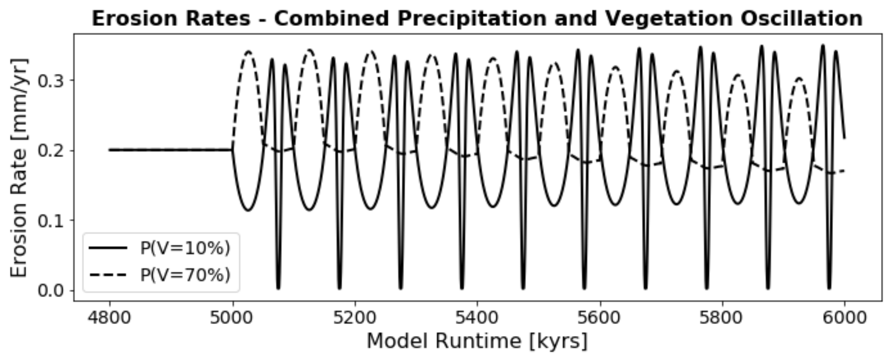

Figure 16 Mean catchment erosion rates for coupled simulations with changes in surface vegetation cover and mean annual precipitation. The first cycle in the time series is expanded in Figure 17.

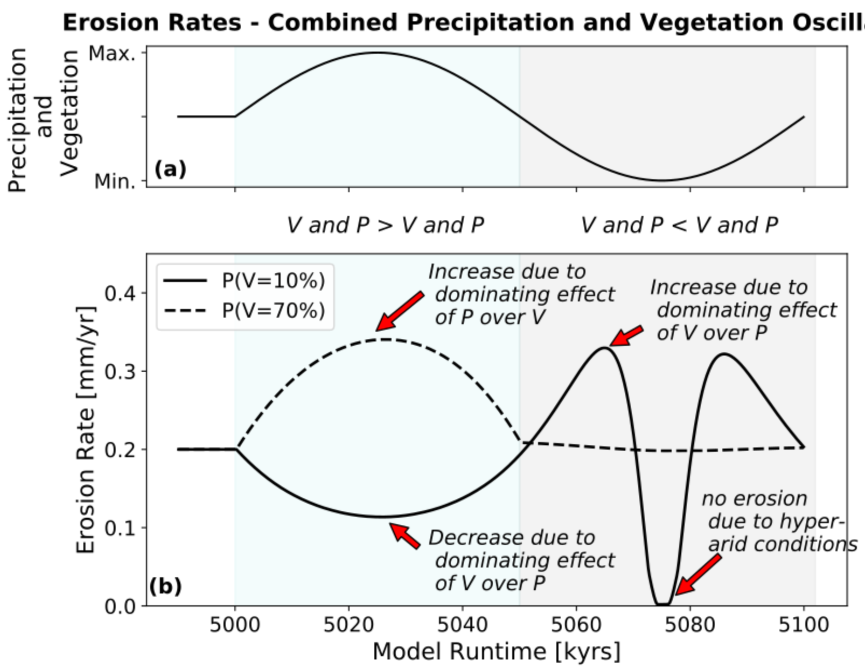

Figure 17 Mean catchment erosion rates for coupled simulations for one period of oscillation after the start of transient conditions (see also Fig. 15). Upper subplot shows conceptualized transient forcing in vegetation cover and mean annual precipitation, lower subplot shows erosion rate for simulations with low (black line) and high (dotted line) initial vegetation cover and precipitation values.

Earth Surf. Dynam. Discuss., https://doi.org/10.5194/esurf-2018-13
Manuscript under review for journal Earth Surf. Dynam.
Discussion started: 21 February 2018

Earth Surface Dynamics Discussions

Table 1 Model parameters used for conduction simulation experiments with Landlab model environment.

Model Parameter	Value
Uplift (U), mm/yr	0.2
Base Fluvial erodibility, m/yr (kg m-1 s-2)-p	7.00E-06
Fluvial Threshold Erosion Rate, L/T	4.00E-04
Base Diffusivity Constant, m2/yr	0.02
Vegetation Oscillation Amplitude, %	+- 10%
Mannings Number for fully vegetated conditions , -	0.01
w	1
alpha	0.3
p	1